NTNU
Norwegian University of
Science and Technology

Modeling and control of catenary mooring systems for vessels, oil rigs, and barges

Øystein Aase

Abstract

In this master thesis, an automatic positioning system for moored vessels has been studied. Although there exist dynamic positioning systems for vessels with integrated thrusters, this system will be considering operations where access to these is limited, usually due to shallow waters. Using the mooring system combined with winches onboard, it is possible to distribute forces such that the vessel moves in the desired direction within the limits of the anchor points. In cooperation with Scantrol As we will propose a control system that can be integrated with existing winch control systems. The performance will then be evaluated through realistic simulations of a vessel in operation.

To be able to test the algorithm, a simulator has been developed in Matlab/Simulink. This simulator is divided into four parts, namely guidance, MPC, winch models, and the vessel model. The guidance handles the switching of waypoints when the waypoint tracking mode is switched on. The MPC optimally distributes forces to all winches onboard such that the reference NED coordinate is being tracked. These desired forces are then being converted into angles that the mathematical models of the winches can use as for a reference input. Finally, the resultant forces and moments produced by the winches are being applied to the vessel model. Due to the various vessels types that may be interested in such a system, an adaptive ship model has been developed based on a 3DOF DP-model.

It is important for an operator to be able to measure the states of the mooring lines due to safety reasons. A dynamic mooring model has therefore been implemented so that the operator can easily analyze the behavior of the lines. The model takes tension produced by the winches as input and simulates the behavior when exposed to hydrodynamic effects and tension change. Due to the high complexity, the mooring model will only serve as additional visual functionality for the operator. Many considerations have been taken to ensure safety. The MPC has constraints on tension which handles the possibility of a line breaking. There is also implemented an alarm system that notifies the operator when the vessel exceeds the limits of the anchor points. When this is happening, the operator needs to rearrange the anchor points to continue operation.

The results of this study indicate that the complete system has the desired behavior, in the sense that the vessel can track waypoints specified by the user within certain error limits, even when exposed to environmental disturbances. There are several advantages in using an MPC over the conventional PID controller proposed in the previous work on this system. It is possible to set constraints on the objective function to ensure safety. Another advantage is that the vessel model and the control allocation algorithm can be combined and implemented into the MPC. The predictive ability does also come in handy when optimal decisions need to be executed.

Sammendrag

I denne masteroppgaven er det blitt utviklet et automatisk posisjoneringssystem for fortøyde fartøy. Selv om det finnes flere dynamiske posisjoneringssystemer for fartøy med integrerte thrustere på markedet, vurderes kun operasjoner der tilgangen til disse er begrenset, vanligvis ved operasjoner på grunt vann. Ved å bruke fortøyningssystemet kombinert med vinsjer ombord, er det mulig å fordele kreftene slik at fartøyet beveger seg i ønsket retning innenfor grensene til ankerpunktene. I samarbeid med Scantrol As presenteres det her et styringssystem som kan integreres med allerede eksisterende vinsjkontrollsystemer. Det komplette systemet vil bli testet og evaluert gjennom realistiske simuleringer av et relevant fartøy.

Det har blitt utviklet en simulator i Matlab/Simulink for å kunne teste ut systemet. Denne simulatoren er delt inn i fire deler, nemlig navigasjon, MPC, vinsjer, og fartøy. Navigasjonsdelen håndterer skifting av veipunkter, MPCen fordeler ønsket kraft produsert fra hver vinsj, vinsjene trekker inn eller slipper ut en ønsket lengde wire, mens de samlede krefter og momenter til slutt påføres fartøysmodellen. Grunnet de ulike fartøystypene som kan være interessert i et slikt system, har det blitt fokusert på å lage fartøysmodellen adaptiv.

For en operatør er det svært viktig å kjenne tilstanden til ankerlinjene. Dette for å kunne opprettholde sikkerheten ombord. Det har derfor blitt implementert en dynamisk fortøynings-modell basert på metoden "lumped mass method". Denne modellen tar spenningen som produseres av vinsjene som inngangsverdi, og simulerer oppførselen til ankerlinjene når hydrodynamiske effekter og spenningsendringen påvirker over tid. På grunn av kompleksiteten til denne modellen, benyttes den som et tilleggsverktøy for brukeren. Det er blitt tatt flere hensyn for å ivareta sikkerheten. MPCen har begrensninger på maks spenning som kan produseres av hver enkelt vinsj, og reduserer dermed risikoen for at en ankerlinje ryker under operasjon. Det er også blitt utviklet et alarmsystem som varsler operatøren når fartøyet overskrider grensene for ankerpunktene. Når dette skjer må operatøren om-plassere ankerpunktene for å kunne fortsette driften.

Resultatene indikerer at systemet fungerer og at båten er i stand til å følge veipunkter spesifisert av operatøren, selv når den blir utsatt for havstrøm. Det er mange fordeler ved å bruke en MPC i motsetning til den konvensjonelle PID-kontrolleren som ble foreslått i det tidligere arbeidet med dette systemet, [2]. Begrensninger kan settes i optimaliseringsproblemet, noe som sørger for at sikkerheten ivaretas ombord, fartøysmodellen og kontrollallokeringsalgoritmen kan begge inkluderes i kontrolleren, og den prediktive evnen til MPCen kan bidra til mer optimale valg.

Preface

This thesis is written as part of a Master's degree in Engineering Cybernetics at the Department of Engineering Cybernetics at the Norwegian University of Science and Technology(NTNU). The project was carried out from August 2017 to January 2018 in collaboration with Scantrol As. The simulator that is proposed in this thesis was developed in Matlab/Simulink. This thesis is based on previous work done in [2]. The student has performed all work independently without any extra equipment or software. Guidance was received from Jan Tommy Gravdahl (NTNU) and Øyvind Hansen (Scantrol As) during the development of the system. Information regarding the vessel, winches, and environment, was obtained through contacts within Ace Winches and Asv Pioneer. All figures presented in the coming sections are either drawn or plotted by the student.

Acknowledgements

I would like to thank Scantrol As for this unique opportunity for welcoming me at their offices. A special thanks go to Øyvind Hansen for his knowledge about Scantrol systems and its customers. I would also like to thank Jan Tommy Gravdahl, for great support and guidance from NTNU.

Øystein Aase
Bergen, January 4, 2018

Contents

List of Figures

List of Tables

List of Acronyms

DP	Dynamic positioning
DOF	Degree of freedom
SDOF	Single Degree Of Freedom
CG	Center of gravity
CO	Center of origin
LOS	Line Of Sight
NED	North, East, Down
GPS	Global positioning system
LOS	Line Of Sight
PID	Proportional, integral, derivative
MPC	Model predictive control
LQR	Linear Quadratic Regulator
QP	Quadratic Programming

Notation

η	Position and attitude vector
ν	Velocity vector
$\mathbf{v}$	Linear velocity vector
ω	Angular velocity vector
$\mathbf{M}$	Mass matrix
$\mathbf{D}$	Damping matrix
τ	Vector of generalized forces
$\mathbf{u}$	Winch inputs
ϕ	Roll angle
θ	Pitch angle
ψ	Yaw angle

Accent	Usage	Description
Tilde	$\eta = \eta - \eta_d$	Error between measures and desired value
Dot	$\dot{\nu}$	Time derivative of the variable
Bold	$\mathbf{M}$	Bold indicates matrix or vector

Chapter 1

Introduction

During the recent years, Scantrol As has received requests for an autonomous positioning system for vessels operating in shallow waters. These vessels are all designed with catenary mooring systems. The catenary mooring system is the most common type of mooring system employed in shallow waters, and the catenary refers to the shape of the line under the influence of gravity. The Asv Pioneer from [17], is an accommodation service barge managed by Dalby Offshore. The barge is equipped with four double drum winches from Ace Winches, [3]. When a change in position is required, the barge is moved by manual regulation. This is a time consuming and expensive operation. The focus in this thesis is therefore to present an alternative automatic positioning system that could be implemented on the Asv Pioneer.

1.1 Dynamic Positioning vs Mooring System

Today, dynamic positioning systems are widely used in the offshore oil industry. For such operations, its is important to keep the vessel at a fixed position with a fixed heading. Dynamic positioning systems automatically control the position and heading of a vessel by using thrusters that are constantly active and balance the environmental forces. These systems offer many advantages, and this is why the market has been growing ever since the first vessel was equipped with a dynamic positioning system in 1961. From [11], historically speaking, the conventional mooring technique was employed for the oil operations long before the dynamic positioning systems where introduced. The use of dynamic positioning systems grew with the increase in water depths and with the exploration in severe environments (the North Sea, followed by cold seas).

Even though dynamic positioning usually is the better option for deepwater operations, mooring systems are still seen as a better option in shallow waters. The investment cost and the increased fuel consumption are the main disadvantages of the dynamic positioning system. It also requires a separate engine room, which is a regulatory requirement. This room is needed to power the thrusters and to provide backup to maintain position in the

case of a fire or flood. A mooring system is not inexpensive either. Cost includes winches, piles or anchors, chains, monitoring devices, as well as devices to locate and collect the anchors. For newbuilt vessels, choosing a dynamic positioning system may be easier than for an already operating vessel. Overall there exist several vessels such as the pioneer, equipped with mooring systems operating in shallow waters. Scantrol As is interested in delivering a positioning system that can be combined with the existing mooring system.
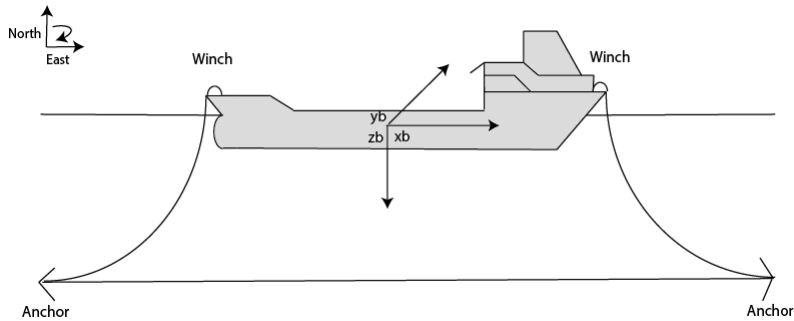
Figure 1.1: Frames of reference

1.2   Problem description

The following subtasks should be addressed:

1. Implement a Model Predictive controller to replace the PID controller and the control allocation algorithm developed in [2].

2. Improve the mooring system analysis proposed in [2] from being a static model to become a dynamical model

3. Include winch dynamics.

4. Perform simulations in Matlab/Simulink in a realistic environment.

5. Conclude your results.

The goal of this thesis is to present a complete control system for stationkeeping and low-speed maneuvering. With a realistic simulator, all vessels that may be interested in the system will be able to verify that it works for their specific operation.

1.3 Contributions

This thesis makes the following contributions:

- Implement a Model Predictive controller to replace the PID controller and the control allocation algorithm developed in [2].

- Improve the mooring system analysis proposed in [2] from being a static model to become a dynamical model

- Include winch dynamics.

1.4 Outline

A literature survey covering the different options of control and mooring for this specific problem is given in Chapter 2. Chapter 3 provides the necessary background material, including reference frames and actuator model. The mathematical models for the vessel, mooring lines, and hydraulic motors are treated in Chapter 4. The Model predictive controller and adescription of the overall control hierarchy are found in chapter 5. Verification of some key parts of the system is found in Chapter 6. The simulator and simulations setup are given in Chapter 7. Simulation results and discussion are treated in Chapter 8. Finally, a conclusion and future work are found in Chapter 9.

Chapter 2

Litterature survey

2.1 Motivation

In the development of a positioning system for moored vessels, several challenges have to be overcome. In particular, the problem is to design a system that can control the position of the vessel with use of winches equipped and also cope with environmental disturbances that may occur. This includes obtaining an algorithm to distribute forces to all winches onboard such that the resultant force vector moves the vessel towards the reference position. The problem can be further extended to modeling and simulate the behavior of the vessel and mooring lines due to the influence of the control system. This chapter serves as a study of the literature and the reasons behind choices that will be presented in the coming chapters.

2.2 Previous work

The previous work on this system is given in the project thesis [2]. The work included an adaptive vessel model based on mathematical models for marine crafts in 3DOF. This model will be further used in the coming sections. The previous work also includes a PID-controller combined with a simple unconstrained allocation algorithm that distributes forces and controls the motion of the vessel. A static model for the mooring lines returns the shape, tension, length, etc. of all lines, which is valuable information for the operator. The complete system is simulated in the Matlab/Simulink environment with external disturbances acting on the vessel. Working close with Scantrol As enabled contact with potential vessels for such a system. The developed control law and vessel model showed promising results and formed the basis for this thesis. However, there is still room for improvements in the system. Introducing MPC and winch dynamics results in a realistic control hierchy.

2.3 Control system analysis

For a vessel such as the Pioneer,[17], the winches onboard have individual systems control-
ling the length of the wires. Since the positioning system needs to coordinate all winches,
this has to be a top-level control system. Multilevel control systems are widely used in
the industry. From section 1 in [19], technological and economical reasons motivate the
development of process plants, manufacturing systems, and traffic networks with an ever
increasing complexity. These large-scale systems are often composed by many interacting
subsystems and can be difficult to control with a centralized control structure due to the
required inherent computational complexity, due to robustness and reliability problems,
and due to communication bandwidth limitations. Scantrol As is interested in proposing
this positioning system on top of the of the already implemented winch control systems.
It is therefore natural to use a hierarchical structure so that the operator easily can switch
between manual and automated control. Another advantage of this structure is the subsys-
tem structure. One faulty subsystem does not necessarily affect the total performance of
the system and may be easily replaced.

From section 5 in [19], in hierarchical multilayer systems, the control action is performed
by some regulators working at different time scales. This can be useful at least in two
cases: when the overall process under control is characterized by different dynamic be-
havior, i.e., by slow and fast dynamics, or in plantwide optimization when optimization
and control algorithms working at different rates compute both the optimal targets and
the effective control actions to be applied. In our case, the regulator acting at lower fre-
quencies computes setpoints to the higher frequency controllers, namely the winch length
controllers. The lower frequency controller has the task of coordinating the winch con-
trollers and ensure that the vessel reaches the destination. Figure 2.1 shows a diagram of
how the system with fast and slow dynamics might look like in our case.

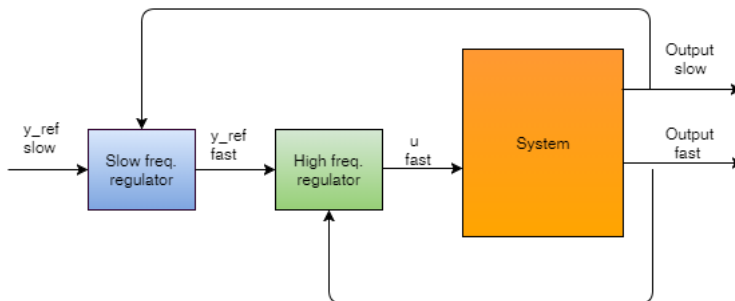**Figure 2.1:** Control of system with fast and slow regulators

The choice of controllers depends a lot on the application. In our case the winches onboard
have one task, to control the angle of the motor shaft. A PID controller can perform this
job. Whether or not all terms in the PID-controller are included, varies from vessel to
vessel. This is due to the importance of accuracy. Choosing P-controllers to control the

angle of the motor shaft on the winches, will, therefore, be sufficient choice for a worst-case behavior of our system. For the low-frequency regulator, two main controllers need to be considered. The Linear quadratic controller (LQR) and the Model predictive controller (MPC) are both based on an algorithm that optimizes the performance over a time horizon. From section 13.1 in [13], the fundamental design problem is the regulator problem, where it is necessary to regulate the outputs $y \in \mathbb{R}$ of the system to zero or a constant value while ensuring that they satisfy time-response specifications. An LQR can be designed for this purpose by considering the state-space model

$$\dot{\mathbf{x}} = \mathbf{Ax} + \mathbf{Bu} \tag{2.1}$$
$$\dot{\mathbf{y}} = \mathbf{Cx} \tag{2.2}$$

The feedback control law for the system is found by minimizing the quadratic cost function

$$\mathbf{J} = \min_u \int_0^T (\mathbf{y^T Q y} + \mathbf{u^T R u}) dt \tag{2.3}$$

where $R = R^T > 0$ and $Q = Q^T \geq 0$ are the weighting matricies. The steady state solution to this problem is

$$\mathbf{u} = -\mathbf{R^{-1} B^T P_\infty x} \tag{2.4}$$
$$\mathbf{P_\infty A + A^T P_\infty - P_\infty B R^{-1} B P_\infty + C^T Q C} = 0 \tag{2.5}$$

where $\mathbf{P_\infty} = \lim_{t \to \infty} \mathbf{P(t)}$. From [16], the idea in MPC is to define a prediction horizon N and approximate the problem with a finite horizon cost

$$J = \sum_{j=k}^{k+N-1} x^T(j|k)Qx(j|k) + u^T(j|k)Ru(j|k) \tag{2.6}$$

The term finite horizon is crucial. It is due to the finite horizon that we can solve the problem., but at the same time, the finite horizon will introduce problems. By using the discretized version of the state space model equation(2.1-2.2), we can predict the state $x(k+j|k)$, given a future control sequence $u(\cdot|k)$ and the current state $x(k|k)$. This gives the prediction

$$x(k+j|k) = A^j x(k|k) + \sum_{i=0}^{j-1} A^{j-i-1} Bu(k+1|k) \tag{2.7}$$

using these predictions, we define the following optimization problem

$$\min_u \quad \sum_{j=k}^{k+N-1} x^T(j|k)Qx(j|k) + u^T(j|k)Ru(j|k)$$
$$\text{s.t.} \qquad u(k+j|k) = \in U$$
$$x(k+j|k) \qquad\qquad = Ax(k+j-1|k) + Bu(k+j-1|k) \tag{2.8}$$

At this point the basic MPC controller is defined by the following algorithm:

Table 2.1: MPC algorithm

MPC Algorithm

1. Meassure x(k—k)
2. Obtain u(*—k) by solving (2.9)
3. Apply u(k) = u(k—k)
4. Time update, k:=k+1
5. Repeat from step 1

It would be in our interest to choose the MPC because of the included constraints. For safety reasons, it is essential to control the tension on each mooring line. If one line breaks, it can cause a possibly deadly situation. The MPC handles this issue inside the optimization problem just by adding a new constraint. And since the time horizon is a moving window, the MPC will update the prediction throughout the simulation time, and therefore also achieve better results than the LQR.

2.4 Mooring system analysis

When an operator is moving his vessel using the winches onboard, the state of the mooring lines is continously being monitoreds. This is due safety reasons. It is therefore of interest to model each mooring line as realistic as possible when the simulations are running. Even though there only a few variables may be controlled by the operator, the visualization part is still of importance. A simulator can be used to verify that the system will work for the specific mooring system.

A mooring line can either be modeled with static equations or with dynamic equations. Previous work has been done in [2], where each mooring line was modeled using static equations. In this thesis we want to extend the mooring analysis and test out the dynamic approach, which is a more realistic way to model each line. Instead of using predefined equations for the behavior, the lines will now change over time when exposed to hydro-dynamical effects. There are multiple ways to implement a dynamic model. From [7], an entirely non-linear time domain analysis is performed. This is a very time-consuming analysis due to all the non-linear effects that need to be accounted for. For this type of analysis, customized software such as DNVGL's Riflex should be used. Since Scantrol As and its potential customers are interested in a mooring analysis, but mostly for visualization purposes, such a model will be too complicated and time consuming, and also not possible to run together with the rest of the simulator.

Consider the SDOF model given in section 2.2 in [9]. The physical properties of linearly elastic structural or mechanical system subjected to an external source of excitation or dynamic loading are its mass, elastic properties, and energy-loss mechanism or damping. In the simplest model of an SDOF system, each of these properties is assumed to be concentrated in a single physical element. Dividing the mooring line into N separate mass elements using the lumped mass method from [6], where each element is modeled as an SDOF system, serves as a good approximation of the behavior of the mooring line. This choice of model is a lot easier to implement, and the also offers a way to control the accuracy by increase/decrease the total number of mass elements. Using a Matlab function to run the dynamic behavior of each mooring line based on external inputs, will work fine together with the rest of the simulator.

Chapter 3

Theoretical Background

The mathematical modeling of a vessel with its associated mooring lines is given in this chapter. This includes reference frames, explanation of notation, and equations of motion.

3.1 Frames of reference

In this thesis we will consider two frames of reference, namely the North-East-Down (NED) coordinate system $\{n\} = (x_n, y_n, z_n)$ and the body-fixed coordinate system $\{b\} = (x_b, y_b, z_b)$. In [13] the NED-frame is defined as the tangent plane on the surface of the Earth moving with the craft, but with axes pointing in different directions than the body-fixed axes. For this system, the x-axis points towards true North, the y-axis towards true East while the z-axis points downwards normal to the Earth's surface. The body frame axes x_b, y_b, and z_b, are chosen to coincide with the principal axes of inertia. This means that x_b is the longitudinal axis, y_b is the transversal axis, and z_b is the normal axis.

3.2 Notation

For a surface vessel operating in 3 Degrees of Freedom (DOF), the following notation from table 2.1 in [13] will be used.

Table 3.1: Degrees of freedom

DOF	Forces/Moments	Linear/angular velocities	Positions/Euler angles
1 motions in the x direction (surge)	X	u	x
2 motions in the y direction (sway)	Y	v	y
3 motions in the z rotation (yaw)	N	r	ψ

which may be convinently expressed in a vectorial setting according to:

$$\eta = \begin{bmatrix} \mathbf{p^n_{b/n}} \\ \mathbf{\Theta_{nb}} \end{bmatrix}, \nu = \begin{bmatrix} \mathbf{V^n_{b/n}} \\ \omega_\mathbf{b} \end{bmatrix}, \tau = \begin{bmatrix} \mathbf{f^b_b} \\ \mathbf{m^b_b} \end{bmatrix} \tag{3.1}$$

where

$$\mathbf{p^n_{b/n}} = \begin{bmatrix} N & E \end{bmatrix}, \mathbf{V^n_{b/n}} = \begin{bmatrix} u & v \end{bmatrix}, \mathbf{f^b_b} = \begin{bmatrix} X & Y \end{bmatrix} \tag{3.2}$$

$$\mathbf{\Theta_{nb}} = \begin{bmatrix} \psi \end{bmatrix}, \omega_\mathbf{b} = \begin{bmatrix} r \end{bmatrix}, \mathbf{m^b_b} = \begin{bmatrix} N \end{bmatrix} \tag{3.3}$$

The superscript and subscripts serves as additional information about the frame. $\mathbf{V^e_{b/n}}$ is read as "The velocity of o_b with respect to $\{n\}$ expressed in frame $\{e\}$".

3.3 Kinematics

Kinematics captures the geometrical aspects of motion. The body frame is a moving frame, and is related to the inertial NED-frame trhough the transformation matricies $\mathbf{R^n_b}(\mathbf{\Theta_{nb}})$ and $\mathbf{T_\Theta}(\mathbf{\Theta_{nb}})$. From [13], the linear and angular velocity transformations are given by

$$\dot{\eta} = \mathbf{J_\Theta}(\eta)\mathbf{v} \tag{3.4}$$

$$\Downarrow \tag{3.5}$$

$$\begin{bmatrix} \mathbf{p^n_{b/n}} \\ \mathbf{\Theta_{nb}} \end{bmatrix} = \begin{bmatrix} \mathbf{R^n_b}(\mathbf{\Theta_{nb}}) & \mathbf{0_{3x3}} \\ \mathbf{0_{3x3}} & \mathbf{T_\Theta}(\mathbf{\Theta_{nb}}) \end{bmatrix} \begin{bmatrix} \mathbf{v^b_{b/n}} \\ \omega^\mathbf{b}_{\mathbf{b/n}} \end{bmatrix} \tag{3.6}$$

where

$$\mathbf{R^n_b}(\mathbf{\Theta_{nb}}) = \begin{bmatrix} c\psi c\theta & -s\psi c\phi + c\psi s\theta s\phi & s\psi s\phi + c\psi c\phi s\theta \\ s\psi c\theta & c\psi c\phi + s\phi s\theta s\psi & -c\psi s\phi + s\theta s\psi c\phi \\ -s\theta & c\theta s\phi & c\theta c\phi \end{bmatrix} \tag{3.7}$$

and

$$\mathbf{T_\Theta}(\mathbf{\Theta_{nb}}) = \begin{bmatrix} 1 & s\phi t\theta & c\phi t\theta \\ 0 & c\phi & -s\phi \\ 0 & s\phi/c\theta & c\phi/c\theta \end{bmatrix} \tag{3.8}$$

where $s = sin()$, $c = cos()$, and $t = tan()$. It should be noted that $\mathbf{T_\Theta}(\mathbf{\Theta_{nb}})$ is undefined for a pitch angle of $\theta = \pm 90°$ and does not satisfy the property 2.1 in [13]. Consequently $\mathbf{T_\Theta^{-1}}(\mathbf{\Theta_{nb}}) \neq \mathbf{T_\Theta^T}(\mathbf{\Theta_{nb}})$. For surface vessel this is not a problem, and since this system is based on surface vessels this does not need to be considered.

3.4 Vessel Parallel Coordinate System

When deriving the linearized equations of motion, it is convenient to introduce a vessel parallel coordinate system obtained by rotating the body axes an angle ψ about the z-axis at each time step [13]. Assumption 7.1 implies that

$$\dot{\eta} = \mathbf{J}_{\Theta}(\eta)\mathbf{v} \approx \mathbf{P}(\psi)\mathbf{v} \tag{3.9}$$

where

$$\mathbf{P}(\psi) = \begin{bmatrix} \mathbf{R}(\psi) & \mathbf{0_{3x3}} \\ \mathbf{0_{3x3}} & \mathbf{I_{3x3}} \end{bmatrix} \tag{3.10}$$

and $\mathbf{R}(\psi) = \mathbf{R_{z,\psi}}$ is the rotation matrix in yaw. The vessel parallel coordinate system is then defined as

$$\eta_{\mathbf{p}} := \mathbf{P}(\psi)^{\mathbf{T}}\eta \tag{3.11}$$

where η_p is the NED position and attitude vector expressed in the body frame and $\mathbf{P}(\psi)$ is given by (3.10). when using linear theory, it is seen that

$$\eta_{\mathbf{p}} = \dot{\mathbf{P}}(\psi)^{\mathbf{T}}\eta + \mathbf{P}(\psi)^{\mathbf{T}}\dot{\eta} \tag{3.12}$$

$$= \dot{\mathbf{P}}(\psi)^{\mathbf{T}}\mathbf{P}(\psi)\eta + \mathbf{P}(\psi)^{\mathbf{T}}\mathbf{P}(\psi)\mathbf{v} \tag{3.13}$$

$$= \mathbf{rS}\eta_{\mathbf{p}} + \mathbf{v} \tag{3.14}$$

where $r = \dot{\psi}$ and

$$\mathbf{S} = \begin{bmatrix} 0 & 1 & 0 & 0 & 0 & 0 \\ -1 & 0 & 0 & 0 & 0 & 0 \\ 0 & 0 & 0 & 0 & 0 & 0 \\ 0 & 0 & 0 & 0 & 0 & 0 \\ 0 & 0 & 0 & 0 & 0 & 0 \\ 0 & 0 & 0 & 0 & 0 & 0 \end{bmatrix} \tag{3.15}$$

For low speed application such as this one, $r \approx 0$. Hence, (3.14) reduces to six pure integrators:

$$\dot{\eta_{\mathbf{p}}} \approx \mathbf{v} \tag{3.16}$$

3.5   Actuator Model

The following theory is gathered from [2]. To be able to control the vessel in 3DOF using static winches onboard, it is necessary to compute the optimal distribution of tension on each winch. By treating each winch as a nonrotatable thruster, this optimal distribution problem can be solved as a known thrust allocation problem. Optimization problems such as this one can be solved using algorithms from the literature.
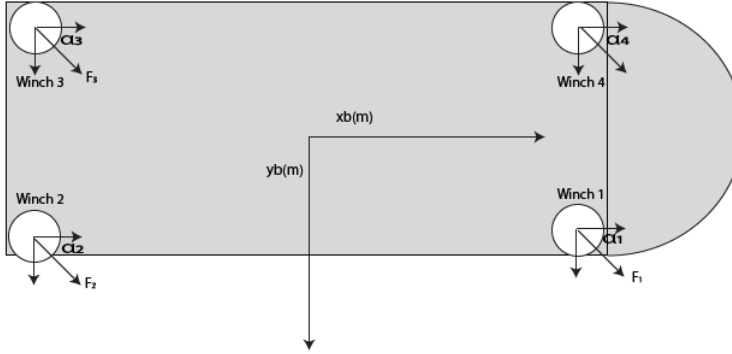

Figure 3.1: Vessel equipped with four winches(forces F1, F2, F3, and F4).The winch forces are decomposed along the x and y axes. From page 403 in [13]

Figure 8.17 serves as a framework for our optimization algorithm. This placement is inspired by [17]. Instead of placing all winches parallel to the x-axis, as in [17], each winch has been separated by $45°$ from the other, such that the vessel can rotate in ψ. It is still possible to use the same frame for different vessels and winch configurations. The winch configuration will be of the following form from (12.237-12.23) in [13].

$$\tau = \mathbf{T}(\alpha)\mathbf{K}\mathbf{u} \qquad (3.17)$$

$$\begin{bmatrix} X \\ Y \\ N \end{bmatrix} = \begin{bmatrix} cos(\alpha_1) & cos(\alpha_1) & \dots & cos(\alpha_r) \\ sin(\alpha_1) & sin(\alpha_1) & \dots & sin(\alpha_r) \\ R_1 sin(\alpha_1) & R_2 sin(\alpha_1) & \dots & R_r sin(\alpha_r) \end{bmatrix} \begin{bmatrix} K_1 & 0 & \dots & 0 \\ 0 & K_2 & \dots & 0 \\ 0 & 0 & \ddots & 0 \\ 0 & 0 & \dots & K_r \end{bmatrix} \begin{bmatrix} u_1 \\ u_2 \\ \vdots \\ u_r \end{bmatrix}$$

$$(3.18)$$

Where $\mathbf{T}$ is the transformation matrix, $\mathbf{K}$ is the gain matrix, $\mathbf{u}$ is the control vector, and τ is the vector of forces and moments. This general configuration frame makes it possible for us to place winches around the vessel at a certain angle α and distance R, and still be able to use the same allocation algorithm.

3.6   Update Winch Angles

The following theory is gathered from [2]. We assume that each winch can be modeled as a nonrotatable thruster. During simulation, the vessel moves relative to the anchor points. This results in a change in the alpha angles. It is, therefore, necessary to update these angles at each timestep. A separate Matlab function takes anchors, winches, and vessel position as input, and returns updated alphas for all winches. This is done in the following manner

Updating the change position

$$dx_i = (N + W_i) - A_i) \tag{3.19}$$
$$dy_i = (E + W_i) - A_i) \tag{3.20}$$

where N and E are the north and east positions of the vessel, while W and A are the winch and anchor positions. The resulting alphas are then computed as follows

$$\alpha_i = atan2(dy_i, dx_i) + \pi + \psi \tag{3.21}$$

where ψ represents the heading angle. Figure 3.2 shows an example of how the winch angles changes while the vessel is moving relative to the anchor points.
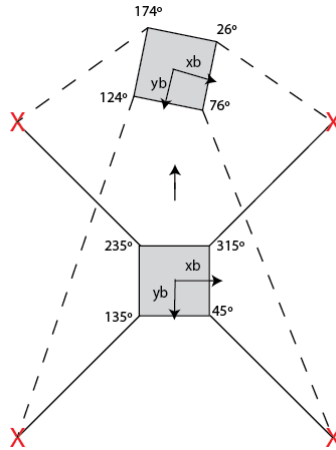
Figure 3.2: Example of change of winch angles during movement

3.7   Waypoint switching

In section 10.3.2 for LOS guidance,[13], Thor I. Fossen proposes a method to switch between waypoints. When moving along a path made up of n straight-line segments connected by n+1 waypoints, waypoint (xk+1,yk+1) can be selected based on whether the craft lies within a circle of acceptance. Moreover, if the craft positions (x,y) at time t satisfy

$$[x_{k+1} - x(t)]^2 + [y_{k+1} - y(t)]^2 \leq \mathbf{R_{k+1}}^2 \tag{3.22}$$

the next waypoint (xk+1,yk+1) should be selected. This strategy will be used to handle this specific issue in the coming simulations.

Chapter 4

Equations of motion

The following sections serve as an explanation to the mathematical models used in the system.

4.1 Vessel model

The following theory is gathered from [2]. The ship model has been carefully chosen to satisfy our specifications. It is reasonable to pick a DP model since mooring systems are low-speed applications, typically 10-30m/min, and easily within the 2 m/s limit for DP models given in section (7.3) in [13]. It is in our interest to control north, east and to head, such that the vessel can move in the north-east frame with the desired orientation. Linear damping is a good assumption for low-speed applications such as this one, and quadratic velocity terms like $\mathbf{C}(v_r)v_r$ and $\mathbf{d}(V_{rc}, \gamma_{rc})$ can also be neglected if we compensate for ocean currents by using integral action. Hence the relative velocity vector v_r is superfluous. From section (7.3.2) in [13], the following linearized DP model for 3DOF is used

$$\dot{\eta_{\mathbf{P}}} = \mathbf{v} \tag{4.1}$$

$$\mathbf{M}\dot{v} + \mathbf{D}v = \mathbf{R}^T(\psi)\mathbf{b} + \tau + \tau_{waves} + \tau_{wind} \tag{4.2}$$

$$\dot{\mathbf{b}} = 0 \tag{4.3}$$

Where $\mathbf{M}$ is the mass matrix, $\mathbf{D}$ is the linear damping matrix, and $\mathbf{b}$ is the ocean currents modeled as a slowly varying bias vector. The right hand side of equation (5.2) represents the external forces and moments acting on the vessel, while equation (4.1) represents the state vectors $v = [u, v, r]^T$ and $\eta = [N, E, \psi]^T$ in parallel coordinates given by the transformation

$$\eta_{\mathbf{P}} = \mathbf{R}^T(\psi)\eta \tag{4.4}$$

where

$$\mathbf{R}(\psi) = \begin{bmatrix} cos(\psi) & -sin(\psi) & 0 \\ sin(\psi) & cos(\psi) & 0 \\ 0 & 0 & 1 \end{bmatrix} \tag{4.5}$$

To be able to implement the suggested DP model, it is necessary to obtain the matrices in equation (5.2). The mass matrix, $\mathbf{M}$, is represented as

$$\mathbf{M} = \begin{bmatrix} m - X_{\dot{u}} & 0 & 0 \\ 0 & m - Y_{\dot{v}} & mx_g - Y_{\dot{r}} \\ 0 & mx_g - Y_{\dot{r}} & I_z - N_{\dot{r}} \end{bmatrix} \tag{4.6}$$

Where m corresponds to the mass of the vessel, I_z is the moment of inertia about the z-axis , x_g is the x-coordinate at the center of gravity, while $X_{\dot{u}}$, $Y_{\dot{v}}$, $Y_{\dot{r}}$, and $N_{\dot{r}}$ are the added mass coefficients. Notice that it is necessary to have some information about the vessel that is being modeled. Scantrol As presented a vessel that is a good candidate and its specifications are given in [17]. Figure 3.2 shows an illustration of the coordinate system used in the following calculations.
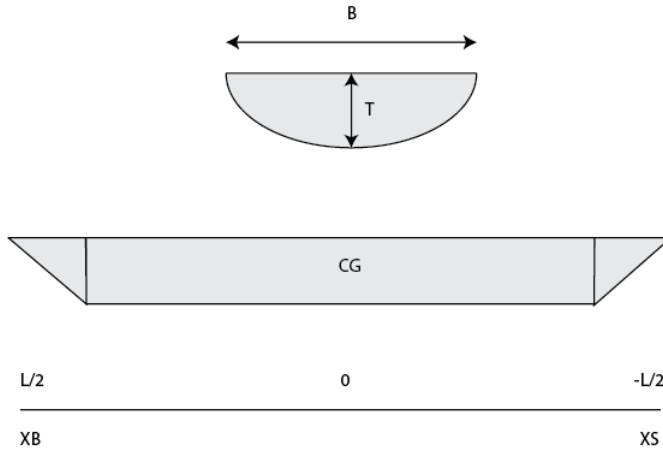

Figure 4.1: Positions of model segments and coordinate system

Using the specifications given in [17], we are able to compute the following parameters

$$m = \frac{1}{2}\rho\pi T^2 L \tag{4.7}$$

$$I_z = \frac{m}{24}(3T^2 + L^2) \tag{4.8}$$

$$x_g = 0 \tag{4.9}$$

These parameters are calculated under the assumption that the hull can be approximated as a half cylinder from strip theory for surface vessels in [12]. We also assume that the center of gravity coincides with the center of origin. T represents the draft of the vessel while L represents the length of the vessel. Both are retrieved from the specifications mentioned above. The final parameter, ρ, represents the water density.

The added mass diagonal coefficients can be computed from equations (2.138)-(2.140) in [12]

$$-X_{\dot{u}} \approx 0.05m \tag{4.10}$$

$$-Y_{\dot{v}} = \frac{1}{2}\rho\pi T^2 L \tag{4.11}$$

$$-N_{\dot{r}} = \frac{1}{24}(0.1mB^2 + \rho\pi T^2 L^3) \tag{4.12}$$

Further on, the linear damping matrix, $\mathbf{D}$, is given as

$$\mathbf{D} = \begin{bmatrix} -X_u & 0 & 0 \\ 0 & -Y_v & -Y_r \\ 0 & -N_v & -N_r \end{bmatrix} \tag{4.13}$$

From section (6.2.1) in [13], it can be assumed for 3DOF maneuvering models that we use a zero frequency model

$$\mathbf{D}_p = B^{1,2,6}(0) = 0 \tag{4.14}$$

This results in a damping matrix dominated by linear viscous damping in the diagonal terms surge, sway, and yaw from section (6.4.1) in [13]

$$-X_u = B11_v = \frac{m + A_{11}(0)}{T_{surge}} \tag{4.15}$$

$$-Y_v = B22_v = \frac{m + A_{22}(0)}{T_{sway}} \tag{4.16}$$

$$-N_r = B66_v = \frac{m + A_{66}(0)}{T_{yaw}} \tag{4.17}$$

Where $A_{ii}(0)$ represents the added mass coefficients, while T_{surge}, T_{sway}, and T_{yaw} represents the chosen time constants. From page 125 in [13], typical values for these time constants lies between 100-250s. we choose $T_{surge} = T_{sway} = T_{yaw} = 150s$. The crossterms $Y_{\dot{r}}$, Y_r, and N_v, are possible to obtain from equations from [8]. In this paper the coefficients are represented as nondimensional values. This means that it is necessary for us to tranform them back to dimmensional values to be able to use them in our model. They are computed from a semi empirical method in equation (25) in [8] as

$$Y_{\dot{r}}' = -\pi \frac{T}{L}^2 (0.67\frac{B}{L} - 0.0033\frac{B}{T}^2)) \tag{4.18}$$

$$Y_r' = -\pi \frac{T}{L}^2 (-\frac{1}{2} + 2.2\frac{B}{L} - 0.080\frac{B}{T}) \tag{4.19}$$

$$N_v' = -\pi \frac{T}{L}^2 (\frac{1}{2} + 2.4\frac{T}{L}) \tag{4.20}$$

and the resulting dimmensional values are given as

$$Y_{\dot{r}} = Y_{\dot{r}}' (\frac{1}{2}\rho L^4) \tag{4.21}$$

$$Y_r = Y_r' (\frac{1}{2}\rho L^3 U_{Net}) \tag{4.22}$$

$$N_v = N_v' (\frac{1}{2}\rho L^3 U_{Net}) \tag{4.23}$$

where $U_{Net} = \sqrt{u^2 + v^2}$ is the net speed of the vessel, which will be updated throughout the simulation. This completes the linearized 3DOF Dp model.

4.2 Static Mooring Model

Floating vessels may drift due to environmental disturbances. To prevent this behavior, many vessels operating in shallow waters are equipped with mooring lines. These lines tie the vessel to the seabed, resulting in a stationary position. A mooring line usually consists of a combination of chain and wire rope, and it is necessary to model the whole line as one unit in response to environmental loads. The mooring line may change its geometry due to hydrodynamic forces, environmental disturbances, or user-defined input at the winch. Tension at the fairlead is an important measure since it represents the force that acts on the vessel. For the overall control system, it is of interest to adjust the tension on all winches, such that the vessel moves in the desired direction. It is also important with tension and angle control to ensure safety. Lines may break at a certain value of tension or anchors might lose grip at a certain angle. We will, therefore, model this behavior to prevent accidents.

An illustration of a mooring line is shown in Figure 4.2. We assume that the seabed is flat and that the line is placed in the x-z plane. It is appropriate to neglect to bending stiffness for chains and wires with a large radius of curvature.
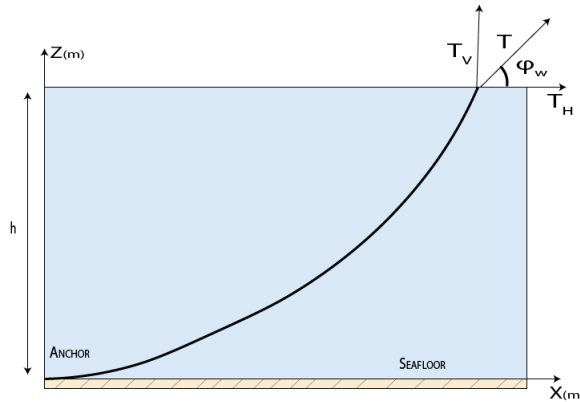
Figure 4.2: Catenary mooring line

From [6], a mooring line can be separated into a finite sum of elements were each element is exposed to hydrodynamic forces. A represents the cross-sectional area of the cable, w is the weight per unit length of the line in the water, while F and D are the mean forces per unit length in the normal and tangential direction, E is the elastic modulus, and T is the line tension. It can be seen that $\rho g z A$ and $\rho g z A + \rho g A dz$ is applied to the endpoints. This because we want the sum of the hydrostatic forces to have a vertical component equal to the weight of the submerged volume of fluid.

The hydrostatic forces is given by

$$dT - \rho g A dz = [w sin(\phi) - F(1 + \frac{T}{AE})]ds \qquad (4.24)$$

$$T d\phi - \rho g A z d\phi = [w cos(\phi) + D(1 + \frac{T}{AE})]ds \qquad (4.25)$$

Equation (4.24-4.25) are nonlinear, and therefore difficult to find a solution. Assuming that we can neglect the hydrodynamic forces F and D and that the line has a constant weight per unit length. This is a good approximation for the static model.
Introducing a new variable for simplification

$$T' = T - \rho g A z; \qquad (4.26)$$

Resulting in

$$dT' = [w sin(\phi)]ds \qquad (4.27)$$

$$T' d\phi = [w cos(\phi)]ds \qquad (4.28)$$

Dividing equations (4.27) and (4.28), we get

$$\frac{dT'}{T'} = \frac{sin(\phi)}{cos(\phi)}d\phi \qquad (4.29)$$

$$T' = T_0' \frac{cos(\phi_0)}{cos(\phi)} \qquad (4.30)$$

By Integrating equation (4.30) we find that

$$s - s_0 = \frac{1}{w}\int_{\phi_0}^{\phi} \frac{T_0'}{cos(\theta)} \frac{cos(\phi_0)}{cos(\theta)}d\theta = \frac{T_0 cos(\phi_0)}{w}[tan(\phi) - tan(\phi_0)] \qquad (4.31)$$

For the static model, the horizontal forces are constant, while the vertical forces change throughout the line. It is therefore only interesting to calculate forces from the seabed and up to the water surface. Choosing s_0 and ϕ_0 equal to zero which simplifies equation (4.30) and (4.31)

$$T' = \frac{T_0'}{cos(\phi)} \qquad (4.32)$$

$$s = \frac{T_0'}{w}tan(\phi) \qquad (4.33)$$

The x-and z-coordinates are possible to find using the following relationship between the streched length dp and the unstretched length ds of a cable element

$$dp = ds(1 + \frac{T}{AE}) \qquad (4.34)$$

Combining this with equations for dx and dz gives

$$\frac{dx}{ds} = cos(\phi)(1 + \frac{T}{AE}) \approx cos(\phi)(1 + \frac{T'}{AE}) = cos(\phi) + \frac{T_0}{AE} \tag{4.35}$$

$$\frac{dz}{ds} = sin(\phi)(1 + \frac{T}{AE}) \approx sin(\phi)(1 + \frac{T'}{AE}) = sin(\phi) + \frac{w}{AE}s \tag{4.36}$$

where the right hand sides are based on equation (2.36) and (2.37). Integrating equation (2.40 from the seabed and up, we find that

$$h = \frac{T_H}{w}(\frac{1}{cos(\phi_w)} - 1) + \frac{1}{2}\frac{w}{AE}l_s^2 \tag{4.37}$$

We know that $cos(\phi_w) = \frac{T_H}{\sqrt{T_H^2 + T_Z^2}}$, and by combining this fact with equation (2.42) to obtain The horizontal tension T_H

$$T_h = \frac{T_Z^2 - (wh - \frac{1}{2}\frac{w^2 l_s^2}{AE})^2}{2(wh - \frac{1}{2}\frac{w^2 l^2}{AE})} \tag{4.38}$$

The vertical tension is given by

$$T_Z = wl_s \tag{4.39}$$

and the total tension T

$$T = \sqrt{T_H^2 + T_Z^2} \tag{4.40}$$

Integrating equation (2.39) in the same way as with equation (2.40) results in the following

$$x = \frac{T_H}{w}log(\frac{\sqrt{T_H^2 + T_Z^2} + T_Z}{T_H}) + \frac{T_H}{AE}l_s \tag{4.41}$$

And by adding the part of the line of the line that lies on the seabed, completes the static mooring model.

4.3 Dynamic Mooring model

Since a mooring line operates in all kinds of weather conditions with external forces acting at all times, the static model is not a good approximation for its behavior. Because of this, we will implement a dynamic model, which takes these forces into account. The following sections, 4.3 and 4.4 are inspired by the work given in [22]. From [9], the essential physical properties of any linearly elastic or mechanical system subjected to an external source of excitation or dynamic loading are its mass, elastic properties(flexibility or stiffness), and energy-loss mechanism or damping. This includes the applied load $p(t)$, the spring force $f_S(t)$, and the damping force $f_D(t)$. The displacement $u(t)$ and the applied load, are positive in the direction of the x-axis. The spring force and the damping force resist the deformation and velocity, hence both act in the opposite direction.
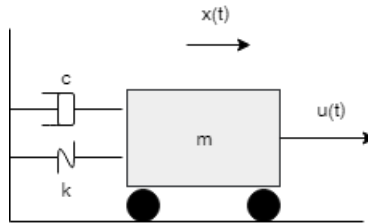

Figure 4.3: Idealized Mass Spring Damper system

The equation of motion for this system is formulated by expressing the equilibrium of all forces acting on the mass using D'Alembert's principle. Since we do have three resisting forces, Newton's second law of motion is given by

$$mu\ddot{}(t) = p(t) - f_S(t) - f_D(t) \tag{4.42}$$

Assuming viscous damping, the damping force f_D becomes a product of the damping constant c and the velocity $\dot{u}(t)$

$$f_D = c\dot{u}(t) \tag{4.43}$$

While the spring force is given by Hooke's law, which i a product of the spring stiffness k and the displacement $u(t)$

$$f_S = ku(t) \tag{4.44}$$

Combining equation (2.47) with (2.48-2.49) results in the final equation of motion for the single degree of freedom system

$$m\ddot{u}(t) + c\dot{u}(t) + ku(t) = p(t) \tag{4.45}$$

This system is also known as the "Mass spring Damper system," Seen in Figure 8.17. This equation can be complicated to solve when $p(t)$ varies with time. A way to handle this problem is to separate the mooring line into a finite number of elements using the lumped mass method.
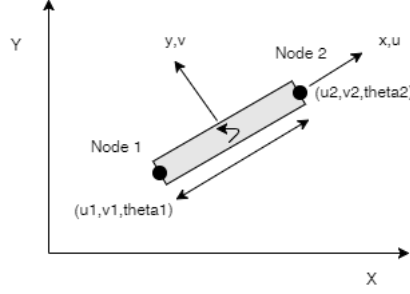
Figure 4.4: Rod element

The parameters of equation (3.50), m,c, and k can be found by approximating each element as a rod moving through water. Such an element is shown in figure 4.4. From [5], the mass and stiffness matrices for a rod with four degrees of freedom are given as

$$
\mathbf{m} = \frac{ml}{2} \begin{bmatrix} 1 & 0 & 0 & 0 \\ 0 & 1 & 0 & 0 \\ 0 & 0 & 1 & 0 \\ 0 & 0 & 0 & 1 \end{bmatrix} \qquad \mathbf{k} = \frac{EA}{l} \begin{bmatrix} 1 & 0 & -1 & 0 \\ 0 & 0 & 0 & 0 \\ -1 & 0 & 1 & 0 \\ 0 & 0 & 0 & 0 \end{bmatrix} \tag{4.46}
$$

The final parameter c, may be modeled as the viscuous damping force from section 6.4 in [13]

$$
c = \frac{1}{2}\rho C_D(R_n)A|u|u \tag{4.47}
$$

where u is the displacement velocity, A is the projected cross sectional area under water, $C_D(R_n)$ is the drag coefficient based on the representative area, and ρ is the water density. The drag coefficient $C_D(R_n)$, is a function of the reynolds number

$$
R_n = \frac{uD}{\nu} \tag{4.48}
$$

Where D is the characteristic length of the body, and ν is the kinematic viscosity coefficient. The problem with equation (4.47) is the nonlinear term $|u|u$. This can be solved using the following approximation

$$
u(\dot{t}_n)^2 \approx u(\dot{t}_n) \cdot u(\dot{t}_{n-1/2}) \tag{4.49}
$$

$$
u(\dot{t}_n) \cdot u(\dot{t}_{n-1/2}) = \frac{u_{n+1} - u_{n-1}}{2\Delta t} \cdot \frac{u_n - u_{n-1}}{\Delta t} \tag{4.50}
$$

Since all variables from the last term on the right hand side of equation (4.49) are known, It is now possible to obtain the approximated damping matrix

$$\mathbf{c} = \frac{1}{2}\rho C_D A \frac{u_n - u_{n-1}}{\Delta t} \begin{bmatrix} 1 & 0 & 0 & 0 \\ 0 & 0 & 0 & 0 \\ 0 & 0 & 1 & 0 \\ 0 & 0 & 0 & 0 \end{bmatrix} \tag{4.51}$$

which completes equation (3.50). From page 192 in [5], the connecttion between local and global displacements are given as

$$\mathbf{v} = \mathbf{T}\bar{\mathbf{v}} \tag{4.52}$$

where

$$\mathbf{v}^T = \begin{bmatrix} v_1 v_2 v_3 v_4 \end{bmatrix} \tag{4.53}$$

$$\bar{\mathbf{v}}^T = \begin{bmatrix} v_1 v_2 v_3 v_4 \end{bmatrix} \tag{4.54}$$

$$\tag{4.55}$$

and

$$\mathbf{T} = \begin{bmatrix} cos(\phi) & sin(\phi) & 0 & 0 \\ -sin(\phi) & cos(\phi) & 0 & 0 \\ 0 & 0 & cos(\phi) & sin(\phi) \\ 0 & 0 & -sin(\phi) & cos(\phi) \end{bmatrix} \tag{4.56}$$

Using the transformation matrix, $\mathbf{T}$, it is now possible to transform equation (3.50) to the global frame in the following manner.

$$\bar{\mathbf{v}} = \mathbf{T}^T \bar{\mathbf{v}} \mathbf{T} \tag{4.57}$$

4.4   Lumped mass method

From [20], the lumped mass method involves lumping effects of mass, external forces, and internal reactions at a finite number of points(nodes) along the mooring line. By applying the equations of dynamic equilibrium and continuity(stress/strain) to each mass, a set of discrete equations of motion is derived. These equations of motion may be solved using finite difference techniques. Material Damping, bending and torsional moments are normally neglected. This procedure implies that the behavior of a continuous line is modeled as a set of concentrated masses connected by massless springs. An illustration is seen in Figure 4.5.

From [9], the lumping procedure is most effective in treating systems in which a large proportion of the total mass is concentrated at e few elements. This is usually the case for mooring lines, where the line is a combination of chain and wire rope elements. For our simulation, we will focus on the vertical and horizontal motion of the line, single degree of freedom(SDOF). The reason for this is that a 6DOF analysis would demand a lot more computational power, and would also not increase the value of this system for the customer. Scantrol As is interested in monitoring the behavior of the line in two dimensions as well as some additional information, such as tension, angles, length, etc. This is achieved using the SDOF system.
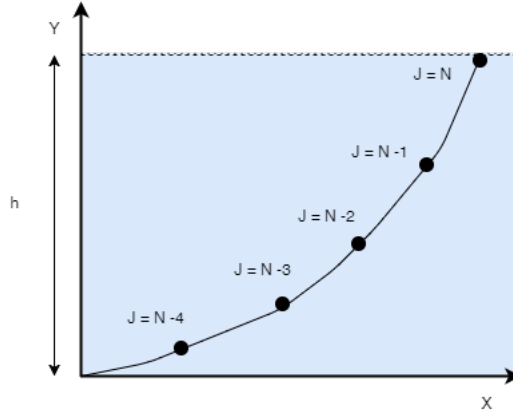
Figure 4.5: Discretized Mooring Line

The procedure starts by choosing the number of elements the line should consist of. From the analytical solution, we find the horizontal force in the line, F_x. We are now interested in finding the vertical force at the start of the line. For the part lying on the seabed, the line has only an axial force. Therefore it is natural to start at the part where the line is lifted from the seabed. The vertical force at this node F_y is expressed as

$$F_{y1} = F_{y0} + \frac{1}{2}w_0 le_1 \tag{4.58}$$

Where le_1 is the length of the element, While we refer to sub-index 0 as the last element on the seabed. Assuming that the element is ideal and has evenly distributed mass. The last term on the right-hand side is due to the lumping of the element mass. Two point masses replace each structural element. The distribution of the two masses being determined by statics. The lumped mass at a node of the structure is the sum of the mass contributions of all elements connected to the node. Since we start our calculations at node 1, this node will only have half the mass from the element that lifts of the ground. We do now have enough information to compute the angle, ϕ_1 and tension, T_1, of element one based on the forces acting on it.

$$T_1 = \sqrt{F_x^2 + F_y^2} \tag{4.59}$$

and

$$\phi_1 = atan(\frac{dx_1}{dy_1}) \tag{4.60}$$

Using the relationship between the stretched length and the unstreched length from (2.38), the coordinates of of node 2 becomes

$$x_2 = x_1 + el_1(1 + \frac{T_1}{A_1 E_1})cos(\phi_1) \tag{4.61}$$

$$y_2 = y_1 + el_1(1 + \frac{T_1}{A_1 E_1})sin(\phi_1) \tag{4.62}$$

With T_1, A_1, and E_1 being the tension, cross section area, and elasticity module of the element. This above procedure is now repeated with the same horizontal force, while the vertical force changes to

$$F_{y2} = F_{y1} + (\frac{1}{2}w_0 + \frac{1}{2}w_2)le_1 \tag{4.63}$$

The lumping of the mass now results in the mass contribution from the elements on both sides of the node. This routine may now be repeated through the entire set of elements, resulting in a complete lumped mass model.

4.5 Hydraulic Motor Model

The position of the vessel is controlled by changing the tension on the winches onboard. Due to this, it is of interest to model each winch. Vessels such as the pioneer are equipped with many winches, either hydraulic or electric. Electric winches are easier to model and have a quicker response than the hydraulic ones. Since there are more hydraulic systems equipped on these vessels, and that such a model will show the worst case performance of the system, hydraulic winches will be considered here.
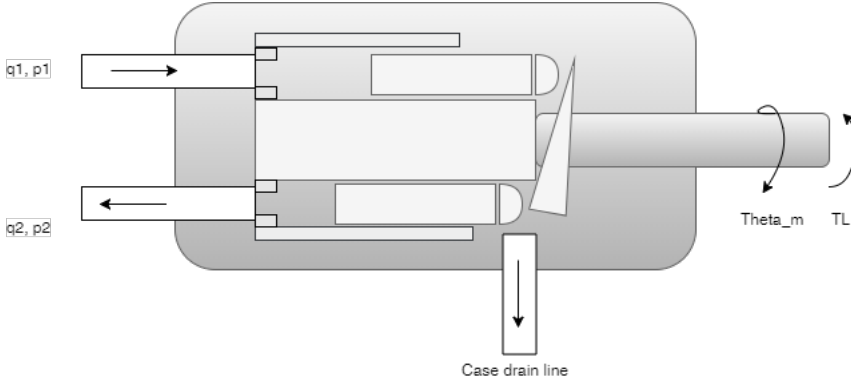

Figure 4.6: Valve controlled hydraulic motor

From section (4.89-4.90) in [10], the hydraulic motor with a matched and symmetric valve is given by the following equations

$$\frac{V_t}{4\beta}\dot{p}_L = -C_{tm}p_L - D_m\omega_m + q_L \tag{4.64}$$

$$J_t\dot{\omega}_m = -B_m\omega_m + D_mp_L + T_L \tag{4.65}$$

Where V_t is the total volume, p_L is the load pressure, and C_{tm} is the leakage coefficient. β represents the bulk modulus, while D_m and q_L are the discharge coefficient and load flow. Finally, J_t is the moment of inertia, B_m is the viscous friction coefficient, T_L is the load torque, and $omega_m$ is the rotational velocity of the motor. A linearized dynamic model for a valve controlled motor is found by inserting the linearized valve characteristics

$$q_L = K_qx_v - K_cp_L \tag{4.66}$$

into the model (4.66-4.67). K_q is here the flow gain, K_c is the leakage coefficient for the valve, while x_v is the spool position.

The complete model of the valve controlled motor is then given by the following three equations

$$\frac{V_t}{4\beta}\dot{p}_L = -K_{ce}p_L - D_m\omega_m + K_q x_v \tag{4.67}$$

$$J_t\dot{\omega}_m = -B_m\omega_m + D_m p_L + T_L \tag{4.68}$$

$$\dot{\theta}_m = \omega_m \tag{4.69}$$

Where $K_{ce} = K_c + C_t m$ is the leakage coefficient for both the motor and the valve and θ_m is the angle of rotation of the motor shaft. Equation (4.69) describes the total mass balance where the flow $K_q x_v$ is input and the load pressure P_L is output. Equation (4.70) describes Newton's second law of rotation as the sum of torques. The output of this function in the acceleration of rotation $\dot{\omega}_m$. The last equation (4.71) is a pure integrator of the angular velocity ω_m, resulting in the angle of rotation θ_m.

Introducing a proportional controller on the spool position, x_v.

$$x_v = K_p(\theta_d - \theta_m) \tag{4.70}$$

With the proportional controller included, it is now possible to control the motor angle based on the desired angle, θ_d. An illustration of the system can be seen in Figure 4.8. From (1.112-4.113) in [10], a rotation motor with matched and symmetric valve that is controlled with a proportional controller will be stable if the velocity constant satisfies

$$K_v = \frac{K_p K_q}{D_m} \leq 2\zeta_h\omega_h \Rightarrow K_p = 2\frac{D_m}{K_q}\zeta_h\omega_h \tag{4.71}$$

A gain margin od 6 dB is achieved with

$$K_v = \zeta_h\omega_h \Rightarrow K_p = \frac{D_m}{K_q}\zeta_h\omega_h \tag{4.72}$$

where ζ_h is the relative damping and ω_h is the undamped natural frequency.
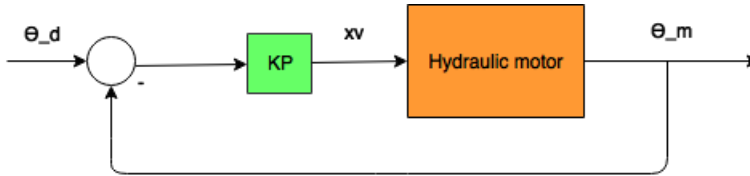

Figure 4.7: Diagram of an hydraulic motor with a P-controller

Chapter 5

Motion Control System

5.1 Control Hierachy

The motion control system is divided into a higher- and a lower order control system. Vessels such as the Pioneer, [17], has mooring systems controlled by winches onboard. Each winch has its control system tracking a reference length given as input by the user. It is, therefore, necessary to add another control layer. This new layer has the purpose of tracking the NED-frame reference and distribute setpoints to the lower level control systems. There are many advantages in dividing a system in this manner. One of the main advantages is the subsystem architecture. Introducing a new control layer on top of the existing ones is usually cheaper than replacing a complete system. If an error occurs in the top layer of the system, the vessel could still be able to move manually. The adaptivity is probably the greatest advantage of this structure. Scantrol As wants to deliver a system to different vessel types with all kinds of mooring systems. With this structure, it is no problem to add or remove a lower level control system component, without affecting the performance of the system.

The performance of such a system depends on the sampling frequency. To ensure stability, the sampling frequency of inner control loop should be higher than the outer control loop. The reason for this is that it is more critical that the winches converge fast to a stable state than for the higher order system.
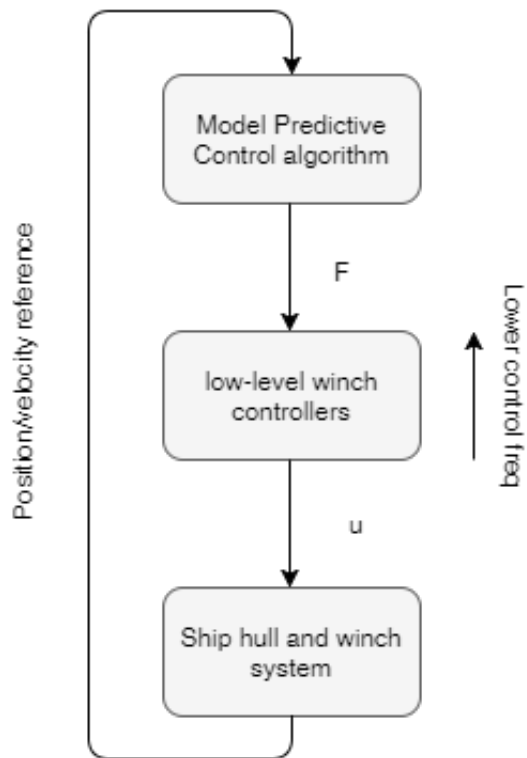
Figure 5.1: Control Hierachy

5.2   Model Predictive Control

The state feedback model predictive control(MPC) is a control algorithm that attempts to minimize a cost function with respect to the modeled system dynamics and constraints on the state and control variables. Using MPC as a high-level motion control algorithm has the advantage that it results in a segmentized software architecture. From Figure 5.1 it can be seen that the MPC obtain setpoints for the lower-level controllers, but runs less frequently.
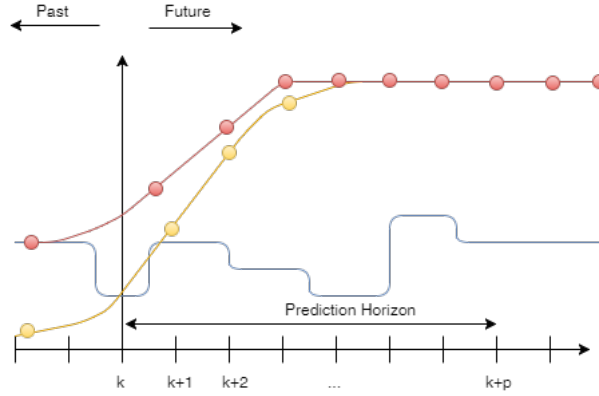
Figure 5.2: Discrete MPC scheme

From [21], the MPC simulates the future behavior of the system it controls and based on the simulation results, attempts to find a control output that makes the system behave optimally. As mentioned before, it is crucial that tension on each mooring line does not cross a certain threshold due to the risk of a line breaking. With an MPC, this problem will be solved by implementing tension constraints on all winches. Restating the motion of the vessel From section 2.7-2.9

$$\dot{\eta_{\mathbf{p}}} = \mathbf{v} \tag{5.1}$$

$$\mathbf{M}\dot{v} + \mathbf{D}v = \mathbf{R}^T(\psi)\mathbf{b} + \tau + \tau_{waves} + \tau_{wind} \tag{5.2}$$

$$\dot{\mathbf{b}} = 0 \tag{5.3}$$

We get the following continuous-time numerical optimization formulation proposed as a basis for the model predictive control

$$
\begin{aligned}
\min_{f} \quad & \mathbf{J}^* = \int_0^{Te}(||\mathbf{f}||)^2_{Qf} + (||\nu||)^2_{Q\nu} + (||\eta_{\mathbf{P}}||)^2_{Q\eta_p} + (||\int_0^{Te}\eta_p dt||)^2_{Qf}dt \\
\text{s.t.} \quad & (\mathbf{T}^\dagger)^{-1}\mathbf{f} = \tau \\
& 0 \leq \mathbf{f} \leq \bar{\mathbf{f}} \\
& \mathbf{M}\dot{v} + \mathbf{D}v = \mathbf{R}^T(\psi)\mathbf{b} + \tau + \tau_{waves} + \tau_{wind} \\
& \dot{\eta_{\mathbf{P}}} = \mathbf{v} \\
& 0 = \tau(\mathbf{Te})
\end{aligned}
\tag{5.4}
$$

Where $\mathbf{f}$ is the resulting forces on all winches from (2.43) and the last term in the objective represents the terminal cost. The weighting matrices $\mathbf{Q_f}$, $\mathbf{Q_\nu}$, and $\mathbf{Q_{\eta_\mathbf{P}}}$ are all positive semi-definite.

5.2.1 ACADO

ACADO Toolkit is a user-friendly toolkit written in C++ for automatic control and dynamic optimization. ACADO is of interest because it offers a great framework for formulating and solving optimization problems. Since ACADO delivers a MATLAB interface, It is easy to combine the MPC with the existing MATLAB/Simulink system. One of the key functions of ACADO is the code export functionality, which generates a library with C functions allowing much faster calculations.

ACADO solves the optimization problem from(2.47) by using a QP solver. More information about the way this solver works in details can be read in the manual, [4].

Chapter **6**

System Verification

This chapter serves as a validation of each new component added to the overall system. This includes the MPC controller, the dynamic mooring model, and the hydraulic winches. Based on realistic parameters gathered from the ASV Pioneer and its mooring system, each component will be tested to verify that it works as expected.

6.1 Verification of Mooring model

The mooring model consists two parts. First, the static mooring model is being computed so that the initial state of the line is given. From this point on, the state is used as input to the dynamic mooring model, which runs through numerous time steps. Here we have external forces constantly acting on the elements of the line. To be able to verify that the models work as we expect, several tests of both models should be performed individually. Starting with the static model, which is based on the equations given in section 4.2.

6.1.1 Static mooring model

By assuming that the equations are proven to work, the best way to verify that the model is implemented correctly is to either change the properties of the line elements or to increase/decrease the tension at the fairlead. Figure 6.1 shows the initial shape of a mooring line consisting of a combination of chain and fiber rope with the given parameters in Table 6.1.

Table 6.1: Mooring line paremeters

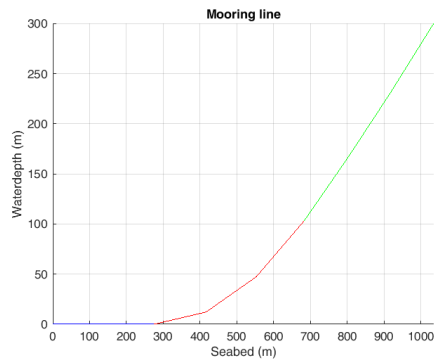| Parameter	Value
Chain elements	6
Fiber elements	3
length chain	700m
length fiber	400m
Weight chain	936
Weight fiber	0.00016872
E chain	211000
E fiber	5027.2
A chain	0.013616
A fiber	0.02745066500

.

Figure 6.1: Initial shape of mooring line with chain and fiber rope

From figure 6.1, it can be seen that the mooring line has the catenary shape where a considerably large part of the line lies on the seabed. Continuing to test whether the line behaves realistically, the tests mentioned above is run. The first plot in Figure 6.2 shows the mooring line shape with increased chain weight,$w = 0.001329$, and with decreased chain weight,$w = 0.000736$. The second plot in figure 6.3 shows the mooring line shape with increased tension,$T = 1.5$, and with decreased chain weight,$T = 0.6$.
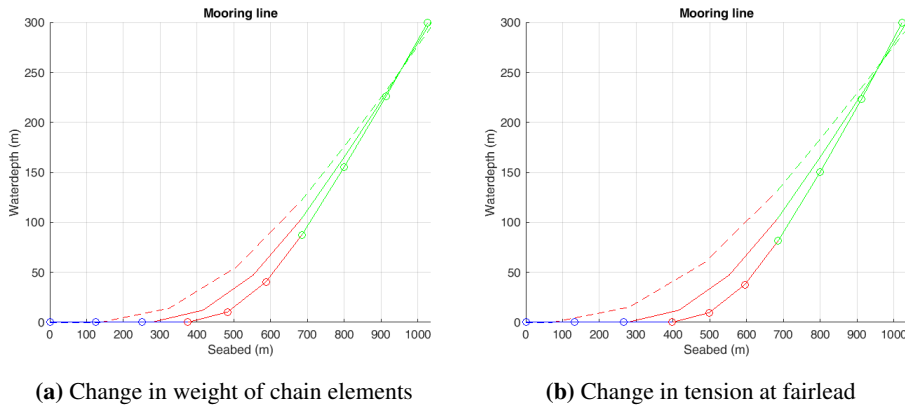

(a) Change in weight of chain elements   (b) Change in tension at fairlead

.   .

Figure 6.2: Verification tests for the static mooring model

By inspecting Figure 6.2, we see that increased chain weight causes result in increased amount of line at the seabed. We can also notice that the angle at the fairlead now is steeper. The opposite happens when we decrease the weight. Since we do have chain elements not just at the lowest part initially, this result is as we could expect. Heavier elements above the seabed cause more of the line to sink down. For the second plot, a similar response is seen. This is because we now are pulling at the fairlead causing the line to be lifted, while the opposite happens when we release tension at the fairlead. The static model seems to be working as expected and can be used further in the dynamic model.
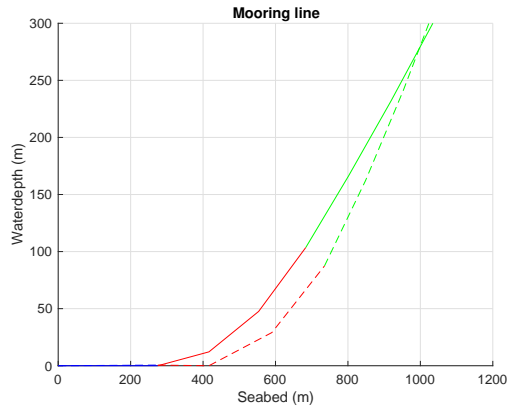
6.1.2 Dynamic mooring model

Figure 6.3: 1 minute simulation of the dynamic mooring model

The dynamic mooring model can be verified by simulating over time and check whether the behavior of the line is stable or not. Simulating with the same parameters given in Table 6.1 for 1 minute resulted in the plot given in Figure 6.3. The dotted line represents the result after the simulation was finished and it can here be seen that line has indeed been exposed to hydrodynamic forces. The dotted line is now lower than the original line. This is due to the forces pushing the line elements towards the seabed. For further inspection, we look at Figure 6.4, which represents the displacement at the end node. Both coordinates experience displacements of about 20 meters in amplitude at the beginning of the simulation but decrease steadily until it reaches approximately 5-10 meters amplitude. Notice that the Y displacement is negative, which verifies the behavior shown in Figure 6.3. We can, therefore, conclude that the line has a stable behavior when we simulate with chosen step size.
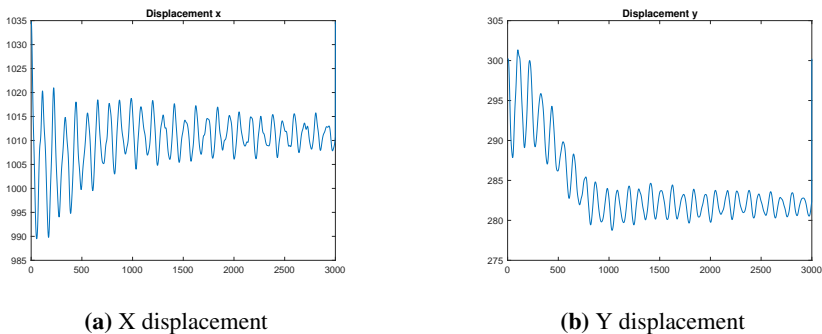

(a) X displacement

(b) Y displacement

Figure 6.4: Displacements during simulation of dynamic mooring model

6.2 Verification of Hydraulic winches

There are four hydraulic winches on the Asv pioneer, each of the type "ACE 100t Double Drum Winches". These winches can be simulated as hydarulic motors given in section 4.5 with the same gear ratio and parameters given in the winch manual [3] and the motor manual [14]. The hydraulic motor model implemented in Simulink is shown in Figure 6.1
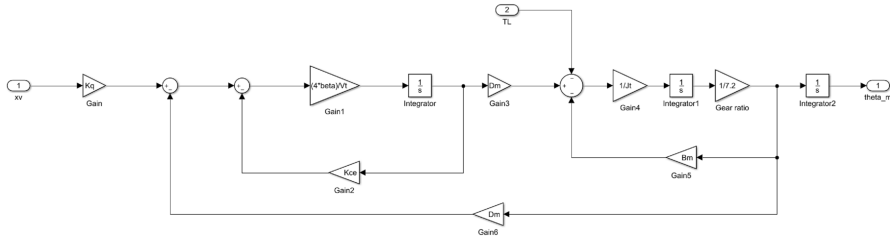

.

Figure 6.5: Simulink diagram of a Valve controlled hydarulic motor

Looking at Figure 6.1, the motor model has a couple of parameters that need to be set for the motor to behave realistically. Notice that the "gear ratio" block corresponds to the gear ratio parameter of 1:7.2 given in the winch manual[3]. The rest of the motor parameters includes the bulk modulus,β, the swept volume of the motor cylinders, Vt, the motor displacement, Dm, the leakage coefficient, Kce, the viscous friction coefficient, Bm, and the moment of inertia, Jt. All these parameters are possible to obtain in the motor manual [14]. Table 6.2 shows the page number in the manual or in the book [10] where the specific parameter is found and the corresponding value converted to desired units.

Table 6.2: Hydraulic motor paremeters

Parameter	Page number in manual/book	Value
β	Book: p432	7e3 bar
Vt	Manual: p5	25.09 l
Kce	Manual: p18	0.0023 l/s bar
Dm	Manual: p5	25.09 l/rev
Bm	Book: p452	0
m	Manual: p9	155 kg
r	Manual p9	1.25 m
Jt	Manual: p9	$mr^2 = 242.19 Kgm^2$

With the parameters set to the values given in the table above, the next step is to tune the p-regulator such that the motor can track a reference angle, θ_d. In Figure 6.2 the motor implemented in Figure 6.1 is packed into the block, "Hydraulic Winch Model".
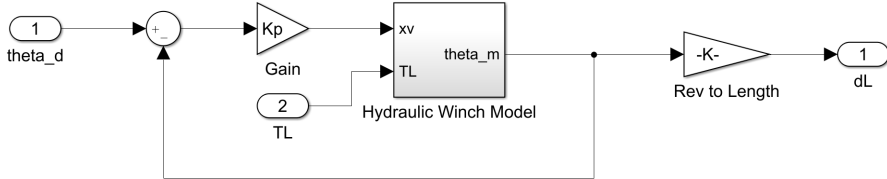

Figure 6.6: Proportional control of the hydraulic winch model

With the chosen units, the input to the motor is θ_d given as a reference number of revolutions. The gain "rev length" is used as a converter from a reference number of revolutions to the length of wire in meters it corresponds to. By trial and error, the $Kp = 5$ and the $Kq = 5$ resulted in the satisfying performance of the controller. Figure 6.3 shows the length of wire the motor produce with $\theta_d = 1$ rev with no load attached. As can be seen, the output has a quick response and is critically damped. This is an important property for the winches since a lack of stability and accuracy will result in errors in the overall system. Since the motor stabilizes at the length of $l = 7.85m$ and the converted input is $l_d = \theta_d \frac{(360)(\pi)(r)}{(180)} = 7.85m$, we can conclude is that the controller is indeed able to track reference input.
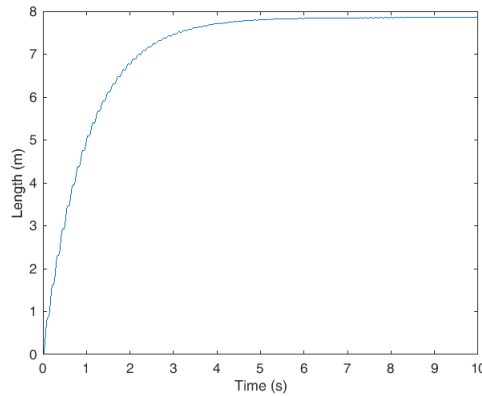

Figure 6.7: Step response for the winch

6.2.1 Spooling factor

A winch that is reeling in wire adds a new layer on top of the drum at each time it reaches the end of the spool. This causes the diameter of the drum to increase and hence the torque arm produced by the motor affected. Therefore it is important to take this into account when a winch is being modeled. Scantrol As has delivered control systems for vessels all over the world and is quite familiar with this problem. Figure 6.4 shows two layers of wire on the winch drum. Assuming that the reeled in wire always will behave as illustrated in Figure 6.4, a like triangle appears. It is then possible to compute the spool factor with basic trigonometry

$$x = dsin(60^o) \tag{6.1}$$

where x is the distance between the layers and d is the wire diameter. Rearanging equation (6.1) gives the spool factor

$$\frac{x}{d} = sin(60^o) \approx 0.87 \tag{6.2}$$

The spool factor given in equation (6.2) is then multiplied with the number of layers,n, and added to the previous torque arm, r_{prev}

$$r_{new} = r_{prev} + nsin(60^o) \tag{6.3}$$

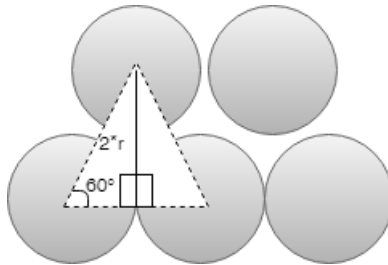$r_n ew$ is the updated torque arm, and is computed at every switch of layer

.

Figure 6.8: Illustration of the added drum diameter due to the spooling factor

Chapter 7

Simulation environment

7.1 Simulator

The simulator is entirely developed in Matlab/Simulink. It is divided into four main parts, the guidance, MPC, winch model, and vessel model. The initialization of the system and all other executions are performed by the main file in Matlab. The Simulink model consists of several Matlab function blocks combined with standard library functions. The conversion blocks between each main block, are based on the static mooring model [18]. These blocks are needed to convert forces given by the MPC into a length which can be used as input on the winches. Since this demands that the static model is run at every single time step, a better way to approach this was to run the model before simulation start and then interpolate the results. This resulted in a linear relationship between the tension and length, which is not necessarily correct. But since the system performed way better way with this interpolation included, this approximation could be accepted. By using the actuator model given in section 3.5, it was possible to combine all forces and moments produced by the winches into a resultant force

The states returned from the Simulink model and the dynamic mooring model should be presented to the user a way that is understandable. Except for basic plots like error and velocity, there has been developed a function that shows the movement of the vessel in the North-East frame based on the Pathplotter function,[15]. An example of such a plot can be seen in Figure 7.1. Visualising the dynamic mooring line can be a difficult procedure. Since we are simulating the lines over a period of time, there are now three dimensions to consider. Using the builtin function plot3 in Matlab, we can monitor the behavior of the lines during simulation. An example can be seen in Figure 7.2. These visual presentations combined with the traditional 2D plots results in a sophisticated simulator environment.
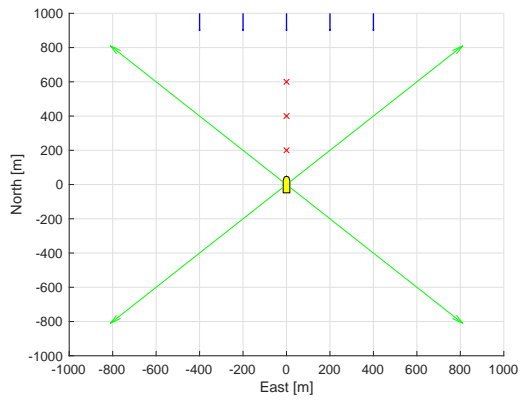
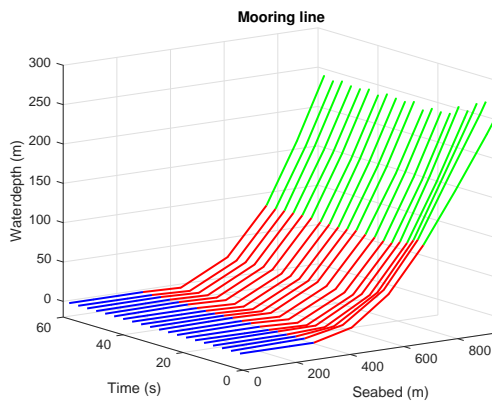**Figure 7.1:** 2D visualization of the vessel with mooring lines

Figure 7.2: 3D visualization of the dynamic mooring model

7.2 Methods of integration

Simulink selects its solver based on the need for accuracy and stability in the system. For our Simulink model, containing MPC, winches, and vessel, the ODE 45 method has been selected. This method uses a variable step Runge Kutta Method to solve the differential equations in the system numerically. The solver is one of the most common solvers offered by Simulink. Based on the resulting outputs from the system, we can conclude that the method is indeed stable. For the dynamic mooring system, we use a different method to obtain the solution. Analytical solution for the single-degree of freedom system as the one given in equation (4.47) is usually not possible to obtain. A way to handle this issue is to use numerical stepping methods.

7.2.1 Central Difference method

From section 5.3 in [6], the central difference method is based on a finite difference approximation to the time derivatives of displacement. This method is explicit for systems with one degree of freedom. Taking constant time steps $\Delta t_i = \Delta t$, the central difference expressions for velocity and acceleration at step i are

$$\dot{u}_i = \frac{u_{i+1} - u_{i-1}}{2\Delta t} \qquad \ddot{u}_i = \frac{u_{i+1} - 2u_i + u_{i-1}}{(\Delta t)^2} \tag{7.1}$$

Substituting these approximations into equation (2.50) gives

$$m\frac{u_{i+1} - 2u_i + u_{i-1}}{(\Delta t)^2} + c\frac{u_{i+1} - u_{i-1}}{2\Delta t} + ku_i = p_i \tag{7.2}$$

Reorganizing equation (4.2) such that u_{i+1} ends up on the left hand side

$$(\frac{m}{\Delta t} + \frac{c}{2\Delta t})u_{i+1} = (\frac{2m}{(\Delta t)^2})u_i - (\frac{m}{(\Delta t)^2} - \frac{c}{2\Delta t})u_{i-1} + p_i \tag{7.3}$$

or

$$\hat{k}u_{i+1} = \hat{p}_i \tag{7.4}$$

Where

$$\hat{k} = \frac{m}{(\Delta t)^2} + \frac{c}{2\Delta t} \tag{7.5}$$

and

$$\hat{p}_i = p_i - (\frac{m}{(\Delta t)^2} - \frac{c}{2\Delta t})u_{i-1} - (k - \frac{2m}{(\Delta t)^2})u_i \tag{7.6}$$

The case where $i = 0$ is also known as the initial conditions and has to be treated seperately

$$u_0 = u_{stat} \tag{7.7}$$

$$\dot{u}_0 = 0 \tag{7.8}$$

Where this results in the system being at ease with the static solution of the mooring line as the initial displacement. Table 7.1 from [6] shows the complete step by step solution for the Central Difference Method

Table 7.1: Central Difference Method

Central Difference Method

1.0 Initial calculations
$\quad$ 1.1 $\ddot{u}_0 = \frac{p_0 - c\dot{u}_0 - ku_0}{m}$
$\quad$ 1.2 $u_{-1} = u_0 - \Delta t \dot{u}_0 + \frac{(\Delta t)^2}{2} \ddot{u}_0$
$\quad$ 1.3 $\hat{k} = \frac{m}{(\Delta t)^2} + \frac{c}{2\Delta t}$
$\quad$ 1.4 $a = \frac{m}{(\Delta t)^2} - \frac{c}{2\Delta t}$
$\quad$ 1.5 $b = k - \frac{2m}{(\Delta t)^2}$

2.0 Calculations for time step i:
$\quad$ 1.1 $\hat{p}_i = p_i - au_{i-1} - bu_i$
$\quad$ 1.2 $u_{i+1} = \frac{\hat{p}_i}{\hat{k}}$
$\quad$ 1.3 If required: $\dot{u}_i = \frac{u_{i+1} - u_{i-1}}{2\Delta t}; \quad \ddot{u}_i = \frac{u_{i+1} - 2u_i + u_{i-1}}{(\Delta t)^2}$

3.0 Repetition for the next step:
$\quad$ Replace i by $i+1$ and repeat steps 2.1, 2.2, and 2.3 for the next step.

7.2.2 Stability

The central difference method is conditionally stable. It will "blow up," giving meaningless results, in the presence of numerical round-off if the time step chosen is not short enough. The specific requirement for stability is

$$\frac{\Delta t}{T_n} = \frac{1}{\pi} \tag{7.9}$$

This is never a constraint for SDF systems because a much smaller time step should be chosen to obtain results that are accurate. Typically, $\frac{\Delta t}{T_n} \leq 0.1$ to define the response adequately

Chapter 8

Simualtion Results

This chapter presents the results obtained by using the mooring system simulator in Simulink. The first part of the results are three basic movements with current acting from a specific angle. The first tests is stationkeeping. The vessel is here supposed to stay in the same position thoughout the simulation. The second test is a straight line maneuver in the North direction, while the third test is a rotation about the origin. The second part of the results contains a more complex prcedure. Based on information retrieved from the Barge Master [1] on the ASV Pioneer, the simulation is set up to to replicate the environment and a typical movement procedure that is performed manually to this day on the Pioneer. Two different sets of waypoints are supposed to be tracked by the vessel. A discusion of the results can be found at the end of this chapter.

8.1 Part I: Basic Maneuvers

This section presents the performance of the system for three basic movements. The tests are chosen specifically to verify that the system can handle basic maneuvers that may be neccessary to excecute during normal procedure. All simulations last for $t = 1000s$. The tests that is being considered are:

Test1: Stationkeeping
Test2: Low speed maneuver, 10 meters North and stationkeep the rest of the simulation
Test3: Rotate 10 degrees about the origin and stationkeep the rest of the simulation

For all the tests above, the vessel has to suppress the disturbance of a constant current attacking from North. To be able to evaluate the performance it is nessasary to simulate all tests in the excact same environment. Therefore, we will use the same vessel parameters, mooring parameters, and winch parameters. These parameters are based on the ASV Pineer and the environment it operates in, and set to the following:

8.1.1 Test 1: Stationkeeping
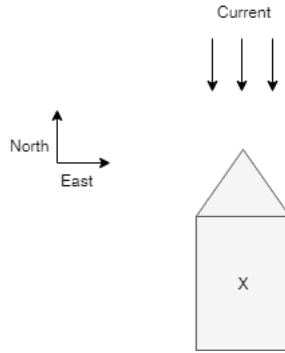
Figure 8.1: Illustration of Test 1

For the stationkeeping test, the vessel should maintain its position at the origin throughout the simulation of $t = 1000s$. When no ocean current is acting on the vessel, we assume that it will successfully station keeps as long as there are no errors in the Mpc controller. For the situation where the ocean current is acting, we assume that the MPC controller can suppress it in a way that makes the vessel able to track the reference input stably.

(a) No current

(b) Current from North
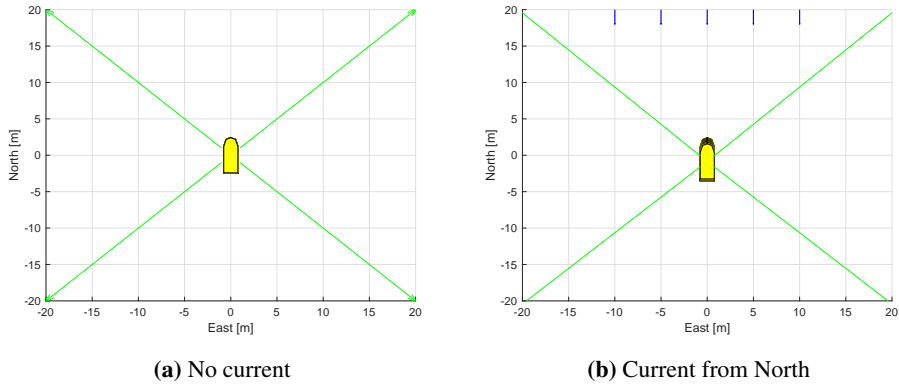
Figure 8.2: Stationkeeping: North-East plot

(a) No current

(b) Current from North
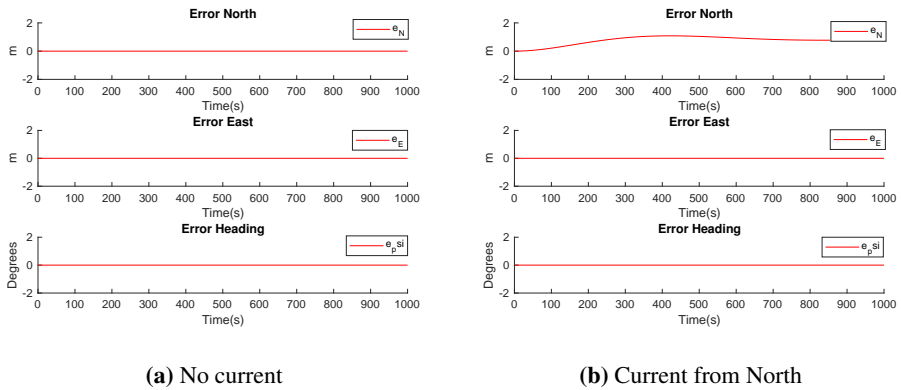
Figure 8.3: Stationkeeping: Error plot

(a) No current

(b) Current from North
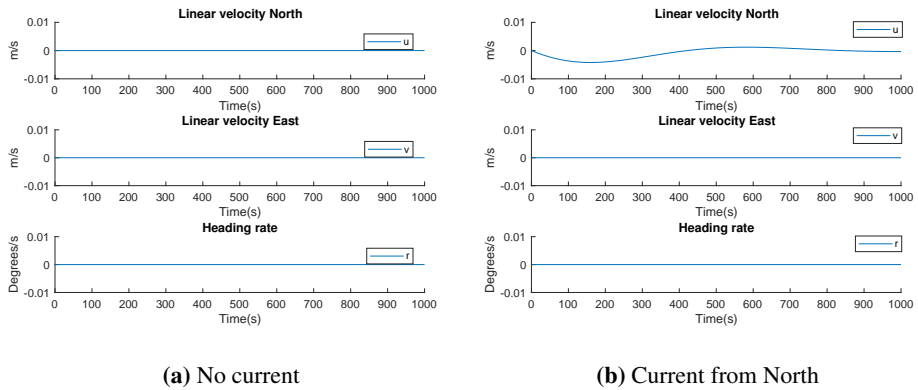
Figure 8.4: Stationkeeping: Velocity plot

8.1.2 Test 2: Low speed maneuver
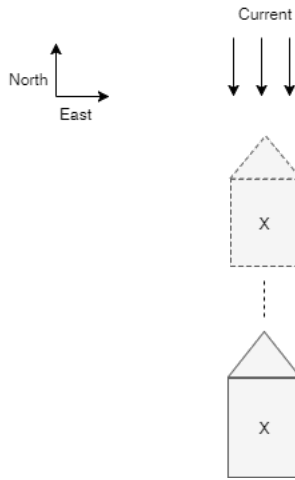
Figure 8.5: Illustration of Test 2

For the low-speed maneuver test, the vessel is supposed to start off at the origin, move slowly towards the coordinate (10, 0,0), slow down, and stationkeeping at this point the rest of the simulation. When no ocean current is acting on the vessel, we assume that the MPC will distribute forces to the winches so that the vessel reaches a constant operational velocity and successfully slows down before it reaches the coordinate. The stationkeeping part for the no current case should be no problem to handle as long as there are no errors in the Mpc controller that results in a nonzero output as mentioned previously. For the situation where the ocean current is acting, we assume that the MPC controller can distribute enough force so that the behavior is similar to the no current case. It should then be possible to track the reference coordinate stably.

(a) No current

(b) Current from North
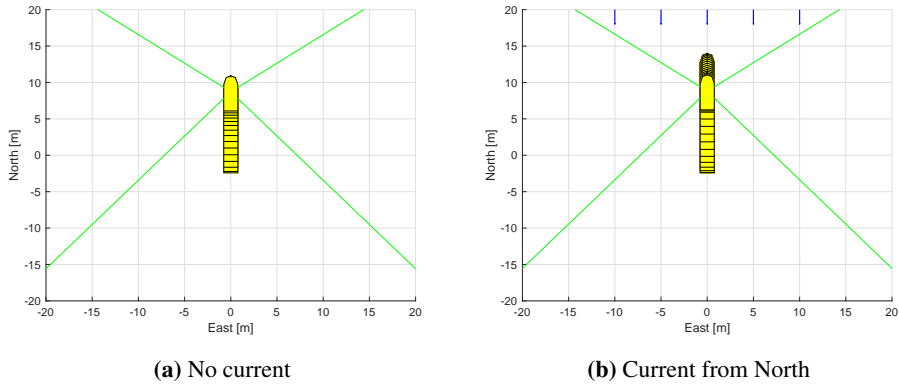
Figure 8.6: Low speed maneuver: North-East plot

(a) No current

(b) Current from North
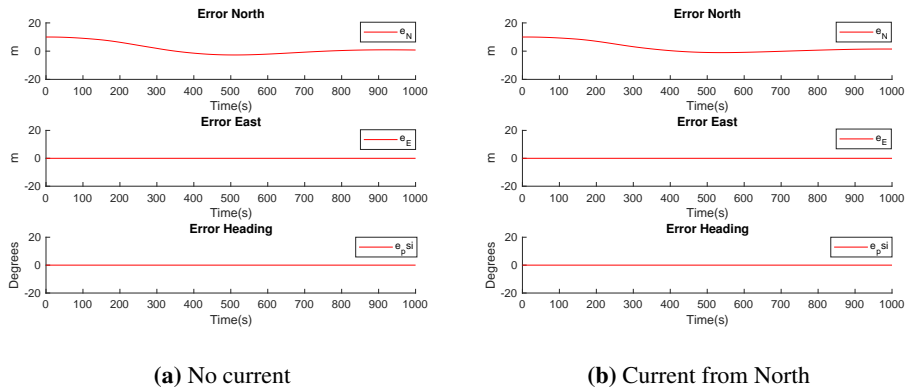
Figure 8.7: Low speed maneuver: Error plot

(a) No current

(b) Current from North
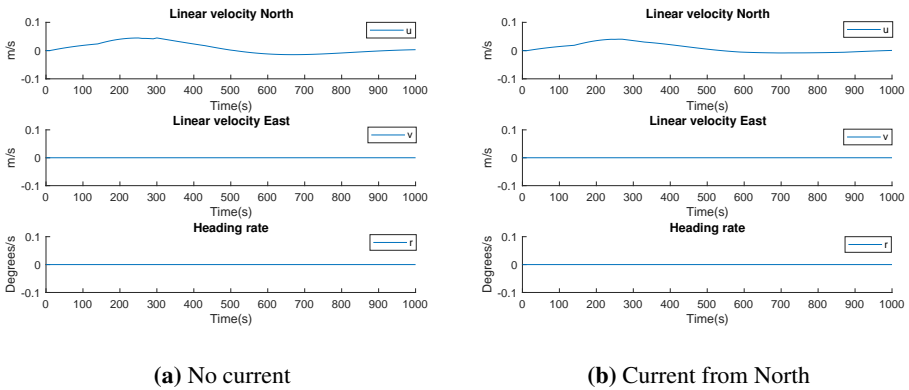
**Figure 8.8:** Low speed maneuver: Velocity plot

8.1.3   Test 3: Rotation
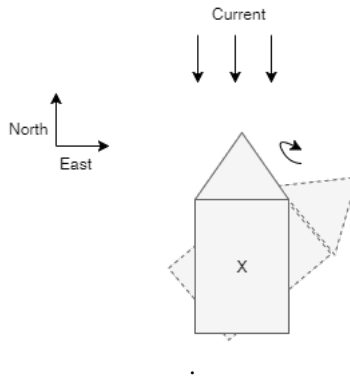
Figure 8.9: Illustration of Test 3

For the rotation test, the vessel is supposed to start off at the origin, rotate slowly towards the coordinate (0, 0,10 degrees), slow down, and stationkeeping at this point the rest of the simulation. When no ocean current is acting on the vessel, we assume that the MPC will distribute forces to the winches so that the vessel can rotate without deviate too much from the origin, and successfully slows down before it reaches the coordinate. The station-keeping part for the no current case should be no problem to handle as long as there are no errors in the Mpc controller that results in a nonzero output as mentioned previously. For the situation where the ocean current is acting, we assume that the vessel should experience some small errors because the current is now hitting the side of the vessel which triggers the cross terms in the Mass and Damping matrices. The vessel should still then be possibly able to track the reference coordinate stably.

(a) No current

(b) Current from North
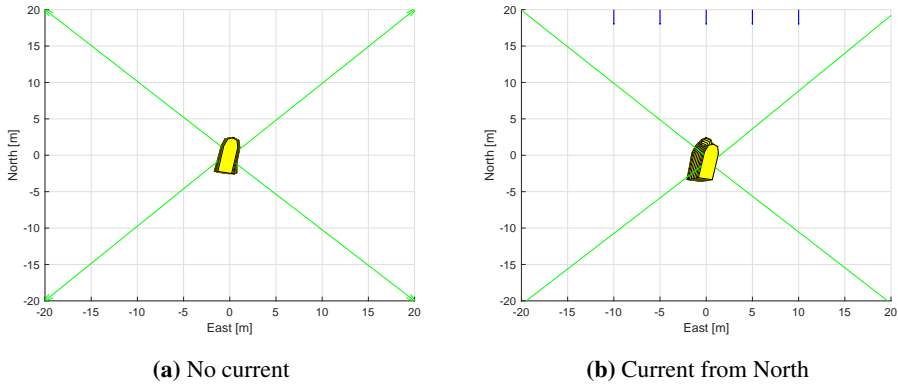
Figure 8.10: Rotation: North-East plot

(a) No current

(b) Current from North
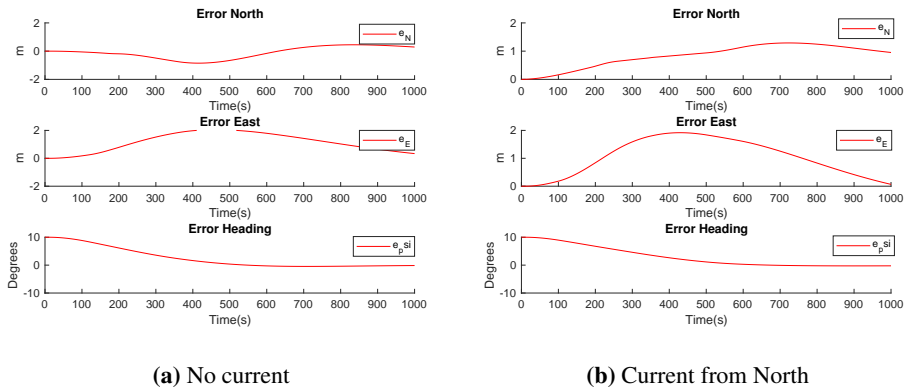
Figure 8.11: Rotation: Error plot

(a) No current

(b) Current from North
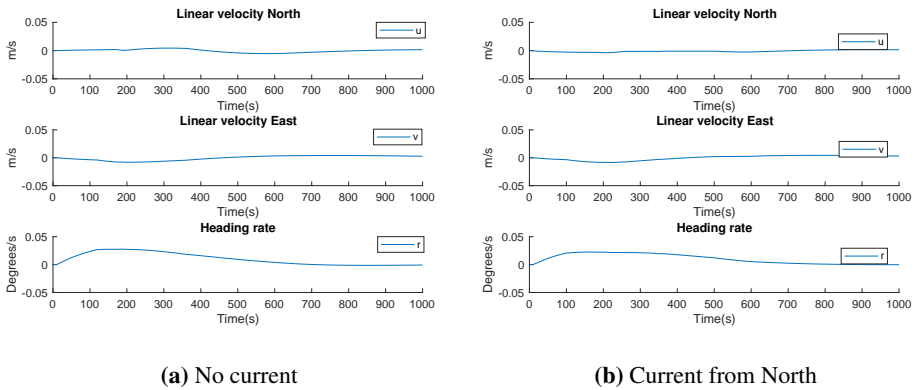
Figure 8.12: Rotation: Velocity plot

8.2 Part II: Waypoint tracking

8.2.1 Scenario A

.
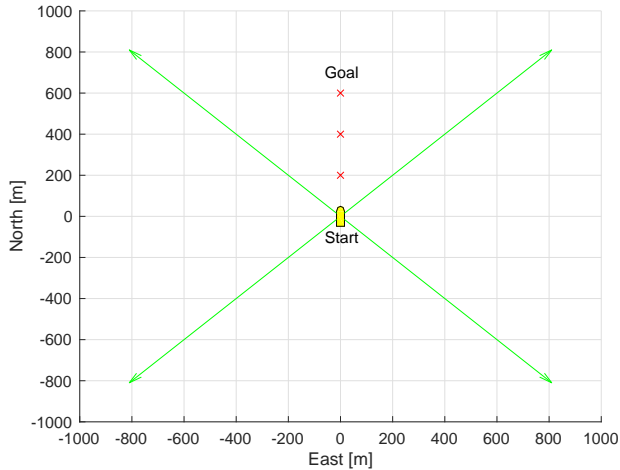
Figure 8.13: Distribution of waypoints Scenario A

For the straight line waypoint tracking Scenario A, the vessel is supposed to start off at the origin, move slowly towards the first waypoint (200m, 0,0). When itFor the straight line waypoint tracking Scenario A, the vessel is supposed to start off at the origin, move slowly towards the first waypoint (200m, 0,0). When it reaches the circle of acceptance for the given waypoint, the vessel should start moving towards the second waypoint at (400m, 0,0). This procedure should continue until the last waypoint is reached for then the vessel to stationkeeping the rest of the simulation. For the situation where the ocean current is acting, we assume that the MPC controller can distribute enough force so that the behavior is similar to the no current case. It should then be possible to track the reference waypoints stably.

(a) No current

(b) Current from North

Figure 8.14: Scenario A: North-East plot

(a) No current

(b) Current from North
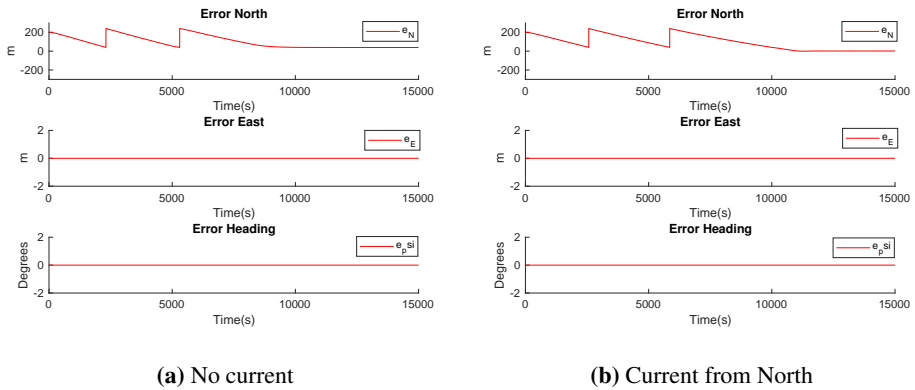
Figure 8.15: Scenario A: Error plot

(a) No current

(b) Current from North
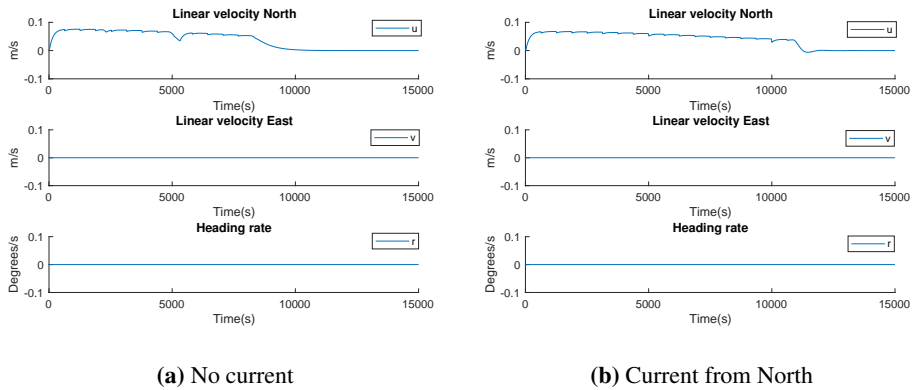
Figure 8.16: Scenario A: Velocity plot

8.2.2 Scenario B

.
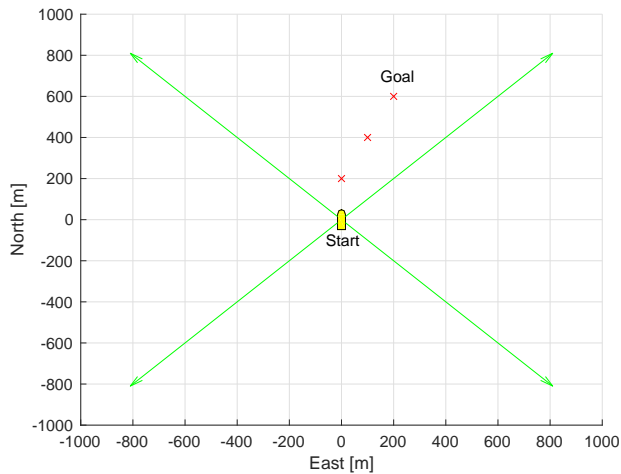
Figure 8.17: Distribution of waypoints Scenario B

For the complex waypoint tracking Scenario B, the vessel is supposed to start off at the origin, move slowly towards the first waypoint (200m, 0,0). When it reaches the circle of acceptance for the given waypoint, the vessel should start rotating before moving towards the second waypoint at (400m, 0,10 degrees). From then on the vessel should continue moving diagonally until the last waypoint is reached for then the vessel to stationkeeping the rest of the simulation. For the situation where the ocean current is acting, we assume that the MPC controller can distribute enough force so that the behavior is similar to the no current case. It should then be possible to track the reference waypoints stably.

(a) No current
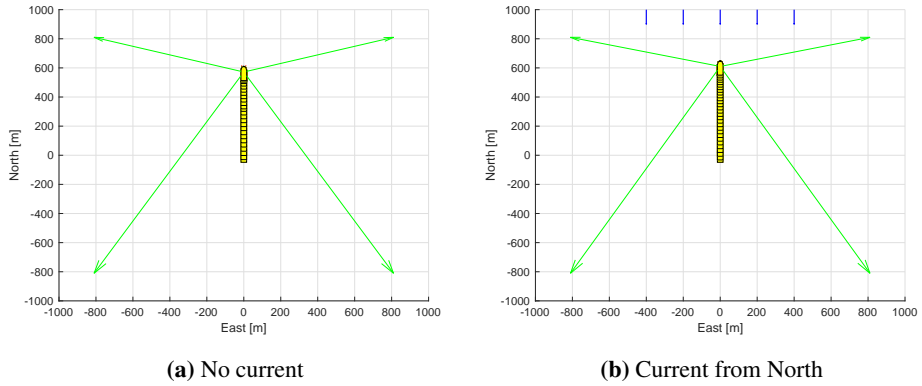
(b) Current from North
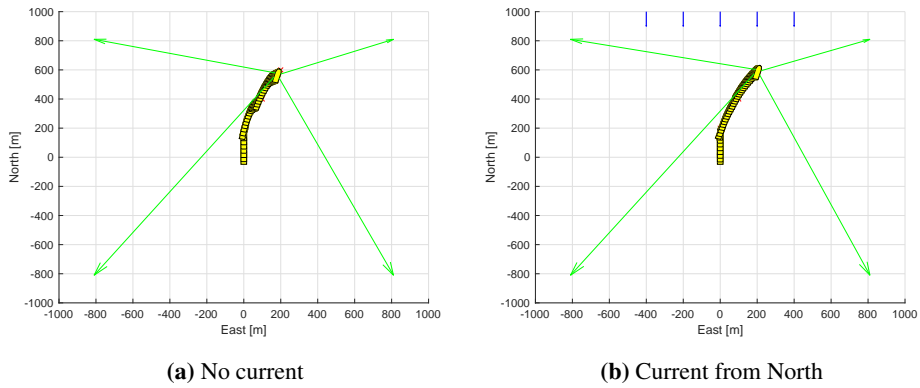
**Figure 8.18:** Scenario B: North-East plot

(a) No current

(b) Current from North
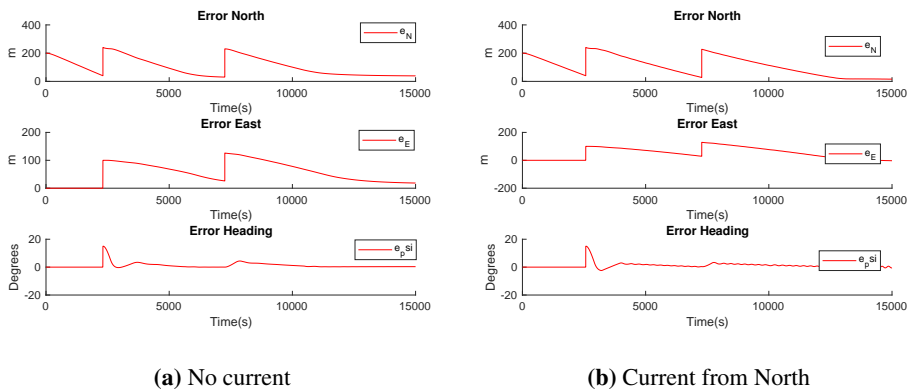
Figure 8.19: Scenario B: Error plot

(a) No current

(b) Current from North

Figure 8.20: Scenario B: Velocity plot

8.3 Discussion

8.3.1 Test 1

The results given for the stationkeeping test shows that the MPC in combination with the winch models is in fact good enough to keep the vessel steady with current acting from North. Looking at Figure 8.2, it is hard to distinct the two plots from each other. Both plots show the vessel at the origin. For a closer inspection, it can be seen in the error plots from Figure 8.3 the vessel with current acting from North is indeed experiencing a small offset. At the beginning of the simulation, the error increases slowly in the North direction until it reaches the maximum at approximately 300 seconds. Looking at Figure 8.4, the velocity is reaching a maximum at approximately 0.05m/s in the south direction before it settles at 0m/s velocity at the end of the simulation. This results in a constant offset of about 1 meter. An error of this scale is not large for the applications that are suggested in this thesis, but an offset should be handled by the disturbance model in the MPC. We expect the MPC controller to predict the incoming current and counteract it so that the vessel stays at the origin. The reason for this behavior is probably due to p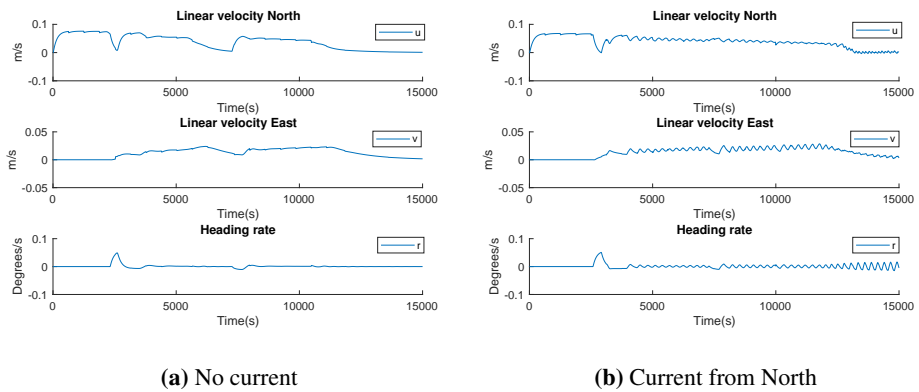oor tuning. Therefore we will experience a small offset, which is not a big deal for the applications presented in this thesis.

8.3.2 Test 2

For the low-speed maneuver, the vessel is supposed to move 10 meters in the north direction, slow down, and stationkeeping until the end of the simulation. Looking at Figure 8.6, it can be seen that the system completes the test without any large errors. Figure 8.7 shows the error during the simulation. We expect the error to start off at 10 meters North, due to the fact the refference is located there. From here on the error decreases for each time step until it settles at around zero at approximately 400 seconds. The results with and without current are very similar, which means that the MPC successfully suppresses the disturbance. Figure 8.8 verifies that the vessel reaches a max velocity at around 0.05m/s and then settles to zero velocity throughout the rest of the simulation. Scaling of the y-axis limits now is larger; it looks like the vessel can stationkeeping without any offset, this is in fact not true. By a closer inspection, we can see that the offset from Performance test 1 at around 1 meter is continuing to affect the system in Performance test 2. It does seem like the system is stable and does the job even with the stationary offset. The velocity is way within the limit of 1 m/s from [13] for the linearized 3DOF DP- model in the North direction and zero for East and Heading.

8.3.3 Test 3

Performance test 3 is a test where the vessel should rotate 10 degrees about the origin and stationkeeping the rest of the simulation. Figure 8.10 shows that the vessel is indeed clockwise rotating before it settles. The error shown in Figure 8.11 is quite interesting. Since the MPC is tuned with a high priority on the heading as seen in Appendix B for both situations, we can see that the controller allows a small error in both North and East direction since it makes the heading error disappear faster. Looking at the heading error, it seems to be decreasing linearly towards zero. Due to the vessel's geometry, a straight line movement demands less force produced by the winches than a rotation about the origin. Looking at the heading error, we see that it settles to zero at approximately 500 seconds and the maximum velocity is reaching approximately 0.025deg/s from Figure 812. The errors in North and East starts decreasing after the heading reaches 10 degrees. At the end of the simulation, all errors seem to settle to the stationkeeping case shown in Performance test 1. Even though there are a few differences in the two situations, the disturbance is being handled, and the vessel reaches its final destination at 10 degrees by the end of the simulation.

8.3.4 Scenario A

For the waypoint tracking case, it is important that the vessel moves from one waypoint to the next with low speed and that the MPC finds a path that does not deviate too much from the straight line path since this would cause the vessel to cross the "cable corridor" given in [1]. The waypoints distribution in Scenario A is shown in Figure 8.13. It forms a straight line in the North direction with a goal at 600 meters. Looking at the results in Figure 8.14, it can be seen that the vessel moves 600 meters before it settles down, both with and without current acting on the system. For a closer inspection, we look at the error plots in Figure 8.15. The error starts off at 200 meters which is correct since each waypoint is separated by 200 meters. The error decreases towards zero, and the vessel reaches the first waypoint at approximately 2000 seconds. The switching algorithm kicks in when the vessel crosses a circle of acceptance, and the next waypoint is set as the reference. This seems to be working well. The second and third waypoints are reached at approximately 5000 seconds and 12000 seconds for the current case. When the last waypoint is reached, the vessel keeps its position throughout the simulation. This is exactly the behavior that we would expect. Figure 8.16 shows that the vessel reaches a maximum velocity close to 0.1 m/s for both situations which are within the limits of both the 1m/s limit from[13] and the operational velocity om 6-8 meters per minutes given in [1].

8.3.5   Scenario B

The last scenario, Scenario B, is a more complex route than what we saw in Scenario A. We have previously seen that the switching of waypoints works as supposed to, but only for a straight line movement. For Scenario B, the vessel is first supposed to move forward until it reaches the first waypoint at 200 meters North. From here on the next waypoints are placed on a straight line 15 degrees from the first waypoint. The waypoint distribution can be seen in Figure 8.17. This specific route tests whether the system is able to keep track on waypoints where the heading is changing during the simulation. By inspecting the results given in Figure 8.18 we can see that the movement is indeed complex. The first thing that is verified is that the vessel settles at the coordinate, 600 meters North and 200 meters East. It can also be noticed that the vessel has a certain heading where the bow points towards the final waypoint. Looking at the error plots in Figure 8.19, we can see that the first waypoint is reached at approximately 2000 seconds, with no error in East or Heading. The second waypoint is reached at approximately 8000 seconds, but now an error of 200 meters North, 100 meters east, and 15 degrees is tracked. Notice that the heading error is prioritized due to the tuning of the MPC. Looking at the velocity plots in Figure 8.20, we see that the vessel reaches approximately 0.1 m/s North before it gets a bump due to the turning of 15 degrees. It is the moving with velocity both in North and in East direction, which is what we would expect. There seem to be some small oscillations in the current case velocity after the first waypoint. This due to the fact that the current now hits the vessel from the side, which is due to the cross terms in the Mass matrix,$\mathbf{M}$, and Damping matrix,$\mathbf{D}$ given in section 4.1. Since the oscillations are small and do not affect the system's overall performance, it is not necessary to dampen it out. The system behaves well in a realistic scenario and visits all the waypoints that are set by the user.

Conclusion and Future Work

This thesis has presented an automatic positioning where the winches onboard are used as actuators. The system can successfully stabilize all 3 degrees of freedom of the vessel model. The goal has been to propose an automatic positioning system for moored vessels. The control system that has been developed can easily be implemented on various types of vessels with moorings systems. The Asv Pioneer and its four point mooring system has been used as a basis for the simulations.

To test the performance and robustness of the control system, a simulator has been developed in Matlab/Simulink. The simulator consists of four parts, namely the Guidance, MPC, Winch models, and vessel model. The Guidance handles the switching of waypoints, the MPC optimally distributes forces to the winches on board, while the winches models reels in/reels out wire according to the desired length given as input. Th resultant forces and moments are then applied to the vessel, resulting in motion. A dynamic mooring model was added as a visual tool so that the operator may observe the behavior of the lines when exposed to hydrodynamic effects and change in tension.

A great deal of effort has been put into testing and verifying the performance of the simulator. To be able to obtain good results, it is necessary to pick realistic parameters in all models included in the simulator. The vessel model is based on the ASV Pioneer specifications, [17], the winch models are based on the hydraulic motor manual, [17], and the winch manual, [3], and the mooring model are based on the mooring line materials in [18]. Several simulations were performed, and the control system was shown to perform well both with and without current acting on the vessel.

The first part of the simulations considered some basic movements, namely stationkeeping, low-speed maneuvers, and a rotation about the origin. It was here shown that the system was stable, but experienced an offset of approximately 1 meter. This offset could probably be handled by tightening the weights in the MPC. The second part of the simulations considered waypoint tracking. Here we tested out two different set of waypoints in

an environment known to the Asv Pioneer. The information was gathered from conversations with the Bargemaster on the Asv Pioneer,[1]. The results showed that the system is indeed able to track waypoints within certain error limits. The MPC finds the optimal path between two waypoints based on the weights set by the operator. The operator can set the weights in the MPC to obtain the wanted behavior of the vessel.

Even though there are still some improvements to be done regarding MPC tuning, it can be concluded that the system has the desired behavior. The Asv Pioneer and several other moored vessels around the world are today moved manually by regulating of the winches onboard. This can easily be avoided by implementing a system such as this one.

Future Work

It is highly recommended for Scantrol As to continue the work presented in this thesis. The simulator serves as a great basis for testing and verification, but a natural next step would be to implement the controller on an operating vessel. To be able to implement a completely working system on a vessel like the Asv Pioneer, some crucial parts needs to be taken care of. The MPC, which is the most important part of the system, needs to be implemented on an embedded system with input from a GPS onboard. It is also necessary to implement some form of control on all winches that is being used such that they can track setpoints given from the MPC. Combining the MPC with the local controllers on-board completes the control system.

The Front-end part of the system is also very important, and should not be underestimated.Therefore it comes in handy that Scantrol As already has tested and delivered a monitoring system for moored vessels. An example of how this specific user interface looks like is given in Figure 9.1. As can be seen, the vessel is centered with its mooring lines. Red/Green indicates whether the tension on the lines are within a critical limit or not. Data such as length, speed, and tension are continuously being updated. Since this monitoring system has most of the properties needed to work with a control system like the one presented in this thesis, it is in Scantrol As interest to combine these two systems into one complete mooring control system. Due to the close relationship with the Asv pioneer and its crew, it would be preferable to test the first version of the system on that specific vessel.

.
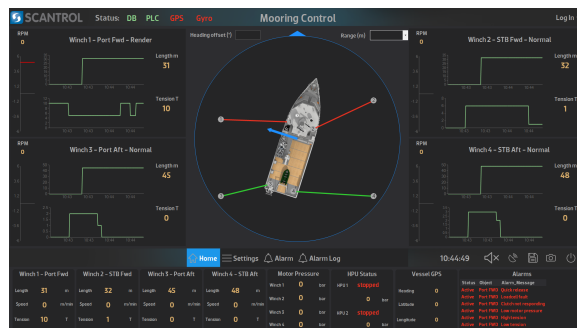
Figure 9.1: Scantrol monitoring system

Bibliography

[1] O. Aase. Conversation with damian breckon. 2017.

[2] O. Aase. Modeling and control of catenary mooring systems for vessel oil rigs and barges. 2017.

[3] ACE-winches. Operations and maintenence manual for ace 100t double drum mooring winches. 2010.

[4] Ariens.D. Acado matlab manual. 2010.

[5] P. Bergan and T. Syvertsen. *Knekking av Syler og Rammer*. Tapir, 1978.

[6] A. Chopra. *Dynamics of Structures (Fourth editon)*. Pearson education,Inc, 2007.

[7] M. Chrolenko. Dynamic analysis and design of mooring lines. 2013.

[8] D. Clarke. The application of maneuvering criteria in hull design using linear theory. 1982.

[9] R. Clough and J. Penzien. *Dynamics of Structures (Third editon)*. Computer & Structures, 2003.

[10] O. Egeland and J. Gravdahl. *Modeling and Simulation for Automatic Control*. Marine Cybernetics AS., 2002.

[11] H. Fay. *Dynamic Positioning Systems: Principles,Design, and Applications*. 1990.

[12] T. Fossen. *Guidance and Control of Ocean Vehicles*. John Wiley and Sons, Ltd, 1994.

[13] T. Fossen. *Handbook of Marine Craft Hydrodynamics and Motion Control*. John Wiley and Sons, Ltd, 2011.

[14] Hagglund. Viking 84-25100 product manual. 1999.

[15] C. Holden. Pathplotter function. guidance and control assignment 3 tasks 2.3-2.8. norwegian university of science and technology. trondheim, norway. 2008.

[16] J. Lofberg. Linear model predictive control stability and robustness. 2001.

[17] D. O. Ltd. Asv pioneer specifications. 2017.

[18] M. OpenCourseWare. Design of ocean systems, lecture 14, mooring dynamics. 2011.

[19] R. Scattolini. Architectures for distributed and hierarchical model predictive control a review. *Journal of Process Control*, 2009.

[20] H. Van den Boom. Dynamic behaviour of mooring lines. 1985.

[21] A. J. B. Veksler and Realfsen.B. Dynamic positioning with model presictive control. 2016.

[22] K. Wingerei. Dynamics and damping in mooring lines. 2008.

Appendix A: Parameters and Constants

MPC

Parameters

Table A1: MPC parameters

Parameter	Value
Ts	0.1s
N	10
Constraint f1	1000N/-1000N
Constraint f2	1000N/-1000N
Constraint f3	1000N/-1000N
Constraint f4	1000N/-1000N

Weights without current acting:
$\mathbf{WN} = diag(1e-1,\ 1e-1,\ 1e-1,\ 1e-3,\ 1e-3,\ 1e-3)$
$\mathbf{W} = diag(1e-2,\ 1e-2,\ 2.5e+3,\ 5e-3,\ 5e-3,\ 5e-3,\ 5e-11,\ 5e-11,\ 5e-11,\ 5e-11)$

Weights with current acting:
$\mathbf{WN} = diag(1e+3,\ 1e+3,\ 1e+3,\ 1e-6,\ 1e-6,\ 1e-6)$
$\mathbf{W} = diag(2.5e+2,\ 2.5e+2,\ 7e+6,\ 5e+1,\ 5e+1,\ 5e+1,\ 5e-7,\ 5e-7,\ 5e-7,\ 5e-7)$

Vessel Model

Parameters:

Table A2: Vessel parameters

Parameter	Value
L	96.56 m
B	30.48 m
T	4.8 m

Constants:

Table A3: Vessel constants

Parameter	Value
g	$9.81m/s^2$
ρ	$1000kg/m^3$
Tsurge	150
Tsway	150
Tyaw	150

Winch placements:

Table A4: Winch placements

Parameter	Value
Winch 1	[15m ,15m]
Winch 2	[-15m ,15m]
Winch 3	[-15m,-15m]
Winch 4	[15m ,-15m]

Anchor placements:

Table A5: Anchor placements

Parameter	Value
Winch 1	[540m, 540m]
Winch 2	[-540m ,540m]
Winch 3	[-540m ,-540m]
Winch 4	[540m ,-540m]

Ocean current

$$\tau_{\mathbf{curr}} = \mathbf{R_t}\mathbf{b} = \begin{bmatrix} -200N \\ 0 \\ 0 \end{bmatrix} \tag{1}$$

where

$$\mathbf{R_t} = \begin{bmatrix} c\psi & s\psi & 0 \\ -s\psi & c\psi & 0 \\ 0 & 0 & 1 \end{bmatrix} \tag{2}$$

Static Mooring Parameters (Conversion blocks)

Parameters:

Table A6: Mooring Parameters

Parameter	Value
D	58mm
w	630.75 N/m
h	30m
AE	302760000 N

Initial horizontal tension:

Table A7: Initial tension Mooring lines

Parameter	Value
Mooring line 1	6244200N
Mooring line 2	6244200 N
Mooring line 3	6244200N
Mooring line 4	6244200N

Appendix B: Matlab Code

The Matlab implementation of the system is distributed over the following m- files, slx-files, and function blocks, which all can be found in the digital attachement:

- – **Run_mooring_system.m**
- – **Mooring_system.slx**
- – **Acado_mpc.m**
- – **MPCfunctionblock**
- – **Vesselfunctionblock**
- – **Dynamic_mooring.m**
- – **Static_mooring.m**
- – **Initiate_winches.m**
- – **Pathplotter.m**
- – **Model_3D_mooring.m**
- – **Compute_winch_angles.m**

The following section presents some key parts of the Matlab code.

Main file

```matlab
1  %Author: ystein Aase
2  tic
3
4  clear all
5  close all
6  %————————————————Mooring parameters
       ————————————————————————
7  T_H1_init = 6244200;
8  T_H2_init = 6244200;
9  T_H3_init = 6244200;
10 T_H4_init = 6244200;
11
12 T_H_init = [T_H1_init ; T_H2_init ; T_H3_init ; T_H4_init ]; %
       Initial tension
13
14 Anchor_1 = [540,540];
15 Anchor_2 = [-540,540];
16 Anchor_3 = [-540,-540];
17 Anchor_4 = [540,-540];
18
19 Anchors = [Anchor_1 ; Anchor_2 ; Anchor_3 ; Anchor_4 ]; %Anchor
       placement
20
21 Winch_1 = [15,15];
22 Winch_2 = [-15,15];
23 Winch_3 = [-15,-15];
24 Winch_4 = [15,-15];
25
26 Winches = [Winch_1; Winch_2; Winch_3; Winch_4 ]; %Winch
       positions from CO
27
28 %%————————————————————Simulation time
       ————————————————————
29 tstart = 0; % Sim start time
30 tstop = 15000; % Sim stop time
31 time = tstart:tstop;%Time
32 delta_t = 0.01; %Sample interval
33 delta_t_mpc = 0.1; %mpc sample interval
34 curr = 0; %Current on/off
35 currangle = 180*(pi/180); % Current angle in NED
36 %————————————————————Waypoints
```

```matlab
37  WP = [200 0 0*pi/180;400 0 0*pi/180;600 0 0*pi/180];%
        timeseries(data,time)';%timeseries(data,time)'; %
        Reference input to simulink
38
39  %% Initiate MPC
40  % ACADO_mpc_working;
41
42  %%Initiate Mooring lines
43  no_elms_bottom = 3;
44  no_elms_above = 3;
45  no_elms_fiber = 3;
46  w_chain = 0.000936;
47
48  minL1 = 100;
49  maxL1 = 500;
50  Tmax = 0.9;
51  for i = minL1:1:maxL1
52      [x,y] =  Static_mooring(i,no_elms_bottom,no_elms_above,
              no_elms_fiber,w_chain,Tmax);
53      h1(i) = max(y);
54  end
55  error = (300-h1).^2;
56  [a, L] = min(error);
57
58  %Run static solution
59  [x_stat,y_stat,Fx,Fy,phi,w,elm_length,A,E,no_elms_total,
        no_elms_chain,no_elms_fiber,no_elms_bottom,T,w_chain,
        w_fiber] = Static_mooring(L,no_elms_bottom,no_elms_above
        ,no_elms_fiber,w_chain,Tmax);
60
61  %Initiate winches
62  % Initiate_winchestest;
63  initiate_winches;
64  Interpolate_static_mooring;
65
66  %%———————————————————Simulation
67  sim Mooring_system2; % The measurements from the simulink
        model.
68  %%
69  %%Time vector
70  t = states.time;
71  %%
72  %%
```

```matlab
73  %States  vessel
74  N =  states.data(:,1);
75  E =  states.data(:,2);
76  psi =  states.data(:,3);
77  u =  states.data(:,4);
78  v =  states.data(:,5);
79  r =  states.data(:,6);
80
81  T1 =  Tension.data(:,1)/(1e6);
82
83  %Error
84  e_N =  error.data(:,1);
85  e_E =  error.data(:,2);
86  e_psi =  error.data(:,3);
87
88  %————————————————————Plot  Path
        —————————————————————————
89  %%
90  tsamp =  100;
91  track =  0;
92  dec =  39000;
93  scaling =  1;
94
95  %%Pathplotter
96  Pathplotter(N, E,  psi, tsamp, dec, tstart, tstop, track,
        WP, scaling, Anchors, Winches, curr)
97  %%
98  % %Dynamic  mooring
99  % Dynamic_mooring_test2;
100 % Model_3D_mooring;
101 %————————————————————Plot  states
        ————————————————————————
102 %
103 figure
104 hold on
105 plot(t, psi*(180/pi))
106 title('Heading')
107 xlabel('Time(s)')
108 ylabel('Degrees')
109 legend('\psi')
110 % ylim([−2  2])
111 hold off
112
113 figure
114 subplot(3,1,1)
```

```matlab
115  hold on
116  plot(t,u)
117  title('Linear velocity North')
118  xlabel('Time(s)')
119  ylabel('m/s')
120  legend('u')
121  ylim([-0.1 0.1])
122  hold off
123
124  subplot(3,1,2)
125  hold on
126  plot(t,v)
127  title('Linear velocity East')
128  xlabel('Time(s)')
129  ylabel('m/s')
130  legend('v')
131  ylim([-0.1 0.1])
132  hold off
133
134  subplot(3,1,3)
135  hold on
136  plot(t,r*(180/pi))
137  title('Heading rate')
138  xlabel('Time(s)')
139  ylabel('Degrees/s')
140  legend('r')
141  ylim([-0.1 0.1])
142  hold off
143
144
145  % % %————————————————————————Plot Error
     ————————————————————————
146  %%
147  figure
148  subplot(3,1,1)
149  hold on
150  plot(t,e_N,'r')
151  title('Error North')
152  xlabel('Time(s)')
153  ylabel('m')
154  legend('e_N')
155  ylim([-300 300])
156  hold off
157
158  subplot(3,1,2)
```

```matlab
159    hold on
160    plot(t,e_E,'r')
161    title('Error East')
162    xlabel('Time(s)')
163    ylabel('m')
164    legend('e_E')
165    ylim([-2 2])
166    hold off
167
168    subplot(3,1,3)
169    hold on
170    plot(t,e_psi*(180/pi),'r')
171    title('Error Heading')
172    xlabel('Time(s)')
173    ylabel('Degrees')
174    legend('e_psi')
175    ylim([-2 2])
176    hold off
177    toc
```

MPC function block

```
1   function T_H = mpc(eta_d , eta , ny)
2   %Author:  ystein Aase
3    %% PARAMETERS SIMULATION
4       T_H = [0; 0; 0; 0];
5       N = 10;
6       n_U = 4;
7       n_XD = 6;
8
9       X0 = [eta' ny'];
10      Xref = [eta_d' 0 0 0];
11      input.x = repmat(Xref ,N+1,1);
12      Xref = repmat(Xref ,N,1);
13      input.od = [];
14
15      Uref = zeros(N,n_U);
16      input.u = Uref;
17
18      input.y = [Xref(1:N,:) Uref];
19      input.yN = Xref(N,:);
20      input.W = diag([0.01 0.01 2500 0.005 0.005 0.005
            0.00000000005 0.00000000005 0.00000000005
            0.00000000005]);
21      input.WN = diag([0.1 0.1 0.1 0.001 0.001 0.001]);
22      state_sim = X0;
23      input.x0 = state_sim(end ,:);
24
25  %Declare patch as extrinsic
26      coder.extrinsic('acado_MPCstep');
27      field1 = 'status';
28      field2 = 'cpuTime';
29      field3 = 'kktValue';
30      field4 = 'objValue';
31      field5 = 'nIterations';
32      info = struct(field1 ,0,field2 ,0,field3 ,0,field4 ,0,
            field5 ,0);
33      fieldx = 'x';
34      fieldu = 'u';
35      mpc_run = struct('info',info ,fieldx ,zeros(11 ,6),fieldu ,
            zeros(10 ,4));
36      mpc_run = acado_MPCstep(input);
37
38      u1 = mpc_run.u(1 ,:)';
39      T_H = T_H + u1;
40  end
```

Vessel model function block

```matlab
function xdot = dp_model_3DOF(x, tau, curr, currangle)
%Author: ystein Aase
%Dp model 3 DOF returns statevector [x, y, psi, u, v, r]

% Check input and state dimensions
if (length(x) ~= 6), error('x-vector must have dimension 6!'); end
if (length(tau) ~= 3), error('u-vector must have dimension 3!'); end

%Constants
g    = 9.81; % acceleration of gravity (m/s^2)
ro = 1000; %Water density (kg/m^3)
Tsurge = 150;
Tsway = 150;
Tyaw = 150;

%Vessel parameters
L     = 96.56;
B = 30.48;          %Pioneer ASV
T = 4.8;
delta = pi*T^2*L;
m = (1/2)*ro*delta;
Iz = (m/24)*(3*T^2+L^2);
xg = 0;
CB = (delta)/(B*T*L);
Unet = sqrt(x(4)^2+x(5)^2);

% %Added mass
X_u_dot = -0.05*m;
Y_v_dot = -(1/2)*ro*delta;
Y_r_dot = -pi*(T/L)^2*(0.67*(B/L)-0.0033*(B/T)^2)*((1/2)*ro*L^4);
N_r_dot = -(1/24)*(0.1*m*B^2+ro*delta*L^2);

% Mass matrix
M = [   m-X_u_dot            0                   0
            0           m - Y_v_dot      m*xg - Y_r_dot
            0         m*xg - Y_r_dot       Iz - N_r_dot];

%Damping
X_u = -M(1,1)/Tsurge;
Y_v = -M(2,2)/Tsway;
Y_r = -pi*(T/L)^2*(-(1/2)+2.2*(B/L)-0.080*(B/T))*((1/2)*ro*
```

```
        L^3*Unet);
42  N_v = -(pi*(T/L)^2)*((1/2)+2.4*(T/L))*((1/2)*ro*L^3*Unet);
43  N_r = -M(3,3)/Tyaw;

44
45  % Damping matrix
46  D = [   -X_u          0          0
47            0         -Y_v       -Y_r
48            0         -N_v       -N_r ];

49
50  % Add current
51  psi = x(3);
52  b = [0; 0; 0];
53  Rt=[cos(psi) sin(psi) 0; -sin(psi) cos(psi) 0; 0 0 1];
54  if curr
55      Rd = [cos(currangle) sin(currangle) 0; -sin(currangle)
            cos(currangle) 0; 0 0 1];
56      b_org = [200 ;0; 0];
57      b = Rd*b_org;
58  end
59  tau_curr = Rt*b;
60  beta = asin(x(5)/Unet);
61   %State space model
62   A = [ zeros(3,3) eye(3)
63         zeros(3,3) -inv(M)*D ];

64
65   B = [zeros(3,3); inv(M) ];

66
67   % Output
68   xdot = A*x + B*(tau + tau_curr);
69  end
```
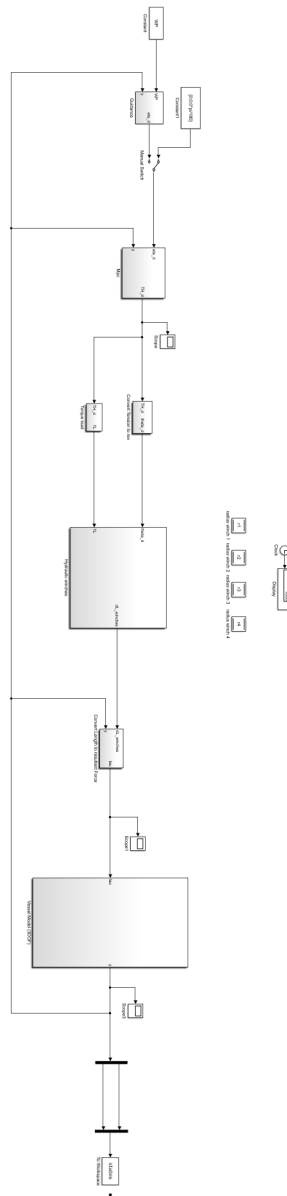
Appendix C: Simulink Model

Figure 2: Simulink model of the system